Cold Atmospheric plasma treatments trigger changes in sun-dried tomatoes mycobiota by modifying the spore surface structure and hydrophobicity

Junior Bernardo Molina-Hernandez, Silvia Tappi, Matteo Gherardi, Riccardo de Flaviis, Jessica Laika, Yeimmy Yolima Peralta-Ruiz, Antonello Paparella, Clemencia Chaves-López

Cold Atmospheric plasma treatments trigger changes in sun-dried tomatoes mycobiota by modifying the spore surface structure and hydrophobicity

Food Control Volume 145, March 2023, 109453

Cold Atmospheric plasma treatment trigger changes in sun-dried tomatoes mycobiota by modifying the spore surface structure and hydrophobicity

Junior Bernardo Molina-Hernandez[a], Silvia Tappi[bc], Matteo Gherardi [d,e], Riccardo de Flaviis[a], Jessica Laika[a], Yeimmy Yolima Peralta-Ruiz[a,f], Antonello Paparella[a], Clemencia Chaves-López[a]*

[a] Faculty of Bioscience and Technology for Food, Agriculture and Environment, University of Teramo, Via R. Balzarini 1, 64100 Teramo, Italy.

[b]Department of Agricultural and Food Sciences, University of Bologna, 47521 Cesena, Italy.

[c] Inter-Departmental Centre for Agri-Food Industrial Research, University of Bologna, via Quinto Bucci 336, 47521 Cesena (FC), Italy.

[d]Department of Industrial Engineering, Alma Mater Studiorum—University of Bologna, Bologna, Italy.

[e]Interdepartmental Centre for Industrial Research in Health Sciences and Technologies, University of Bologna, Bologna, Italy.

[f]Programa de Ingeniería Agroindustrial, Facultad de Ingeniería, Universidad del Atlántico, Carrera 30 Número 8-49, Puerto Colombia 081008, Colombia

* Correspondence: cchaveslopez@unite.it

Abstract

The contamination of sun-dried tomatoes during processing can have a decisive impact on the quality of the finished product. In this study we investigated how Cold Atmospheric Plasma (CAP) under high surface power density (SPD) values can reduce fungal contamination in sun-dried tomatoes. In the application of this innovative processing method, the established "regime" for air plasma chemistry was the transition regime or NOx regime. First, we isolated and identified the mycobiota present on the tomatoes surfaces by mean of the analysis of the ITS region. The analysis revealed 32 different species, with *A. niger*, *A. tubingensis, A. chevalieri*, *A. flavus,* and *A. alternata* being the most abundant. Then, to reduce the fungal population, CAP-NOx was applied for 5, 10, 20 and 30 min on the surface of dried tomatoes. After incubation for 10 days, we observed that the antifungal effect was species and dose-dependent. *In vitro* investigation on the most abundant species revealed that *A. chevalieri* PSJ144 was the most sensitive species (almost 90%) immediately after 5 min of CAP treatment. With the increase of the exposure time up to 30 min, a strong reduction ($p \leq 0.05$) of spore germination of *A. alternata* PSJ77 and *A. tubingensis* PSJ100 was observed (98 and 92%, respectively). However, spores of *A. niger* PSJ38 and *A. flavus* PSJ30 showed the highest resistance to the treatment.

Moreover, the reparameterized Weibull function allowed to obtain useful information about germination kinetics as a function of time of CAP-NOx treatment, revealing that the resistance of the spores was: *A. chevalieri*<*A. alternata*<*A. tubingensis*t<A. *flavus*< *A. niger*. *In situ* analyses confirmed a significant effect on natural fungal contamination by CAP-NOx treatment (76.5 % of reduction), likely due to cell membrane rupture and cell death caused by plasma radicals. In addition, Pearson correlation analysis showed that spore resistance was highly correlated ($p=0.98$) with their hydrophobicity. In a nutshell, our results clearly indicate that CAP-NOx treatment is an effective technique to reduce fungal contamination in sun-dried tomatoes. Among non-thermal processing methods, CAP shows promising perspectives of application in the tomato industry, to mitigate the effects of energy price rises.

Introduction

Daily consumption of fruits and vegetables, in sufficient quantity and quality, helps prevent diseases such as cardiovascular diseases, diabetes and cancer, as well as deficiencies of micronutrients and essential vitamins. The World Health Organization (WHO) ranks inadequate consumption of fruits and vegetables sixth among the 20 risk factors for human mortality. Although these products are known to contain a natural non-pathogenic epiphytic microbiota, they can be contaminated with microorganisms that can be pathogens from human and animals, and can grow during harvesting, transportation, processing, and handling.

Tomato (*Lycopersicon esculentum* L. var. Excell and Aranca) is a highly perishable and fragile vegetable, which is highly susceptible to contamination by microorganisms and mechanical damage during transportation, processing, and storage (Hegazy, 2017). They are not only consumed as fresh produce, but also processed into a variety of products, such as pulp, ketchup, sauces, paste, juices, and dried tomatoes (Sanzani et al., 2019). In this context, several strategies are used to produce dried tomatoes. Sun-drying, which is the oldest among all the drying techniques, is still one of the most commonly used methods to produce dried tomatoes. Nowadays, sundried tomato is an important ingredient in the food and catering industry, but the quality of this product is not always constant (Sohail et al., 2011). During production, the fruit is sliced to increase the surface-area to volume ratio for the loss of moisture, and the pieces are then dried in open spaces under the sun, where they can come into contact with microorganisms, dirt, soil and insects, leading to possible microbial contamination of the product (Canakapalli et al., 2022). Tomato slices are left in full sun for 4–8 days until they have lost most of their moisture content up to 10–15% (Oberoi et al., 2007). In Italy, dried tomatoes are first cured with sodium chloride for 7 days, and then stored at room temperature without humidity control, reaching a shelf-life of around 12 months at room temperature. Drying is a critical step in processing, which can lead to fungal contamination from the environment, which can affect the quality of the product (Kakde & Kakde, 2012; Sanzani et al., 2019). In addition, rehydration of dried fruit under unsuitable storage conditions may reactivate the fungal growth with subsequent mycotoxin formation (Karaca et al., 2010). Some studies have reported the presence of fungal spores in dried tomatoes, which belonged to the following species: *Aspergillus flavus, Aspergillus niger, Aspergillus parasiticus, Mucor*

spp., Penicillium brevicopactum, Penicillium chrysogenium, Fusarium culmorum, Aspergillus rugulovalvus formerly *Aspergillus rugulosus* (syn Emericella rugulosa var. lazuline), *A. niger*, *A. amstelodami*, *A. tubingensis, A, cristatus, R. oryzae, Cladosporium cladosporioides, Corynascus sepedonium*, and *Alternaria sp.* (Molina-Hernandez et al., 2022; Sanzani et al., 2019; Suleiman et al., 2017). Among these species, *Aspergillus* ssp., *Alternaria sp*. and *Penicillium* sp. deserve special attention since several species of these genera can produce mycotoxins. The incidence of these toxic fungal metabolites in dried tomatoes results in economic losses for growers as contaminated export products are rejected (Abdallah et al., 2020; Heperkan et al., 2012). Therefore, the industry today uses strategies aimed to reduce the growth of these molds, which are generally based on the use of chemicals. However, the increasing demand for foods with high quality, with less or no additives, promotes the development of technological alternatives for fungal control. In particular, due to the recent rise of energy prices, non-thermal processing methods are appealing options for food manufacturers.

Over the last decades, various non-thermal technologies have been proposed for surface decontamination of dried fruits, including gaseous ozone and ozonated water (Zorlugenç et al., 2008), ultraviolet (UV–C) alone and in combination with clove essential oils (Gündüz & Korkmaz, 2019), pulsed light (PL) (Aguiló-Aguayo et al., 2013), ultrasound (Görgüç et al., 2021), gamma (γ) irradiation (Hamanaka & Chandel, 2009), electron beam irradiation (Mousavi Khaneghah et al., 2020), microwave (Popelář ová et al., 2021), and cold atmospheric plasma (CAP) (Lee et al., 2015; Molina-Hernandez et al., 2022). The latter technology involves the use of a mixture of ionized gas consisting of charged particles, electric fields, ultraviolet (UV) photons, and reactive species, which can exert a strong oxidative power (Laurita et al., 2021). The chemistry that governs the atmosphere inside a plasma reactor depends on the surface power density (SPD), which is the ratio between the power absorbed by the plasma and the surface area of the electrode. According to Simoncelli et al. (2019), two different regimes can be observed below and above a SPD threshold of 0.1 W/cm^2: 1) small SPD values, where the chemistry is dominated by ozone formation reactions (O_3 –regime); 2) high SPD values, where the formation of NO, N, NO_2, NO_3, N_2O_5, O, O_3 dominates, in a condition that is known as transition regime or NOx regime. Few publications have reported the potential antibacterial activity through the generation of Reactive Nitrogen Species (Wang et al. 2022) by plasma treatment (Shaw et al. 2018). Some researchers have been proposed that NO and the production of intracellular derivatives, such as peroxinitrite

and carbonate radicals, can act as effective antimicrobial agents, causing biological effects (DNA damage, binding to iron centers, oxidiation of thiols, cysteine, etc.) that induce permanent damage in microorganisms (Hao et al. 2014).

Recently, we have shown that CAP-O_3 treatments affect the fungal community structure in sundried tomatoes, as fewer fungi were isolated, and their diversity decreased with prolonged CAP treatments (Molina-Hernandez et al., 2022). To the best of our knowledge, there are no studies in the scientific literature on the application of CAP under NOx regime to decontaminate dried fruits. Thus, the aim of this study was to evaluate the effects of CAP at NOx regime on the fungal population on the surface of sundried tomatoes collected in different regions of Italy. First the predominant mycobiota in sundried tomatoes was identified by molecular methods before and after treatment. Next, spore inactivation of the most abundant fungal species, isolated from dried tomato samples, was investigated.

2. Materials and methods

2.1. Samples

Twenty-three batches of sundried tomatoes (2 kg) were randomly collected from retailers across Abruzzo, Puglia, and Umbria regions in Italy during March 2021. All samples were of commercial quality; samples were selected to avoid visible damage or macroscopic contamination by filamentous fungi. To avoid fungal development without affecting the viability of spores present in sundried tomato, samples were stored in vacuum packed at 20°C until analysis.

2.2 Natural mycobiota in sundried tomatoes

2.2.1. Fungal isolation

For each batch, ten sundried tomato fruits were randomly selected for each treatment and for the untreated control. For the control and after the treatments, each fruit sample was cut into squares of approximately 1.5 x 1.5 cm, and subsequently the different sub-samples were aseptically placed on different culture media: Potato Dextrose Agar (PDA), Malt Extract Agar (MEA), Nutrient agar (WL), and Dichloran Glycerol agar base (DG18) for xerophilic filamentous fungi. Chloramphenicol (0.05 g L^{-1}), purchased from Liofilchem (Liofilchem, Roseto degli Abruzzi-Italy), was added to all culture media with to prevent bacterial growth. All Petri dishes were

incubated for 7 to 10 days at 25°C with 12 h of light and 12 h of darkness in a humid chamber. The plates were then examined to measure the percentage of colonized sub-samples, and fungal diversity (morphotypes). The different colonies were tentatively identified according to their morphology (Samson, Hoekstra and Van Oorshot, 1984) and grouped by their morphological appearance. Pure cultures were obtained from hyphal tip transfer to PDA media and stored at 5°C. The percentage of frequency of each morphotype (MF) for each treatment was calculated according to:

$$MF\ (\%) = (\sum \text{isolates of the morphotype})/(\sum \text{all fungal isolates}) \times 100$$

Finally, to increase the rate of fungal growth, the plates were incubated at 30°C.

2.2.2. Phenotypical and molecular identification of filamentous fungi

To identify the isolates based on the morphological and growth characteristics, single colonies were purified in malt extract agar (MEA) (Liofilchem, Roseto degli Abruzzi-Italy), and subsequently isolated filamentous fungi were identified based on the morphological characteristics under a light microscope according to Munitz et al. (2013). Then, the fungal isolates were tentatively assigned to different genera based on the size and shape of the spores and mycelia. To confirm the identity of the fungi, molecular identification was then carried out according to the method reported by Delgado-Ospina et al. 2021. The PCR assay was performed using the primers listed in Table 1. The ITS region was amplified with the primer pair ITS1-ITS4, ITS1-ITS2. Additional loci (β-tubulin, Calmodulin) were used to identify *Aspergillus* species. All primers used were purchased from Sigma Aldrich (Saint Louis, Missouri, USA).

Table 1. Primers used for PCR assay.

Gene name	Gene	Length bp	Primer	Sequences (5´→ 3´)	Reference
Internal transcribed spacer 1 (ITS1) and ITS2 regions and the 5.8S ribosomal DNA (rDNA) region	**ITS (1-4)**	420-825	ITS1 (F)	**5´TCCGTAGGTGAACCTGCGG3´**	(Glass & Donaldson, 1995)
			ITS4 (R)	**5´TCCTCCGCTTATTGATATGC3´**	
	ITS (1-2)	565-613	ITS1 (F)	**5´ GGAAGTAAAGTCGTAACAAGG 3´**	
			ITS2 (R)	**5´ TTGGTCCGTGTTTCAAGACG 3´**	

β-tubulin	**ben A**	1125	β-tub 2a (F)	**5´GGTAACCAAATCGGTGCTTTC 3´**	(Makhlouf et al., 2019)
			β-tub 2b (R)	**5´ACCCTCAGTGTAGTGACCCTTGGC 3´**	
Calmodulin	**cmdA**	543	Cmd5 (F)	**5′-CCGAGTACAAGGAGGCCTTC-3′**	
			Cmd6 (R)	**5′-CCGATAGAGGTCATAACGTGG-3′**	

Abbreviation: F: Forward, R: Reverse

2.3. Plasma Treatments

A detailed description of the plasma system used for the treatments has already been given in a previous work (Molina-Hernandez et al., 2022), but the most relevant details are reported here for the sake of completeness. Cold Atmospheric Plasma (CAP) was generated by a Surface Dielectric Barrier Discharge (SDBD) placed at the top of a closed chamber, defining a confined atmosphere. A high voltage generator produced a sinusoidal waveform with a peak voltage of 6 kV and a repetition frequency of 23 kHz; the power density absorbed by the plasma source was of 425.35±25.79 W, resulting in a surface power density of 2,6 W/cm^2. Treatments were carried out at room temperature (26 ± 1 °C). Thirty sundried tomato pieces were placed side and successively treated as described in paragraph 2.2.1. Afterward, the plate with the samples was subjected to CAP treatment at 20 cm perpendicularly from the SDBD.

2.4. Optical Absorption Spectroscopy (OAS) measurements

OAS measurements were performed as described by Simoncelli et al. (2019). More specifically, OAS measurements rely on the Lambert-Beer law, which correlates the amount of light absorbed by a certain species to the absolute concentration of such species:

$$n_k = -\frac{1}{L\sigma_k}\ln\frac{I}{I_0}$$

where n is the concentration of the *k-th* species, L is the optical path (25 cm), I_0 is the intensity of incident light, and I is the residual light intensity after the absorption.

The wavelengths selected for the absorption measurements performed in this study and the absorption cross-sections of the absorbing species of interest, O_3 and NO_2, are listed in Table 2. These wavelengths were defined, in accordance with Moiseev et al. (2014), to maximize the absorption of the molecules while minimizing the contribution, and thus the interference from other absorbing molecules.

Table 2. Absorption cross-sections in cm^2 of the species of interest at each selected wavelength.

Selected wavelength	O_3 cross-section	NO_2 cross-section
253±1.2 nm	(1,12±0.02) E-17	(1.1±0.3) E-20
400±1.2 nm	(1,12±0.08) E-23	(6.4±0.2) E-19

The setup conditions used to perform the OAS were the same described by Simoncelli et al. (2019). Two LEDs were used as the light source, one with maximum emission at 255 nm and the other with maximum emission at 400 nm. The light beam was focused using optical fibers and fused silica lens to obtain a parallel beam passing inside the plasma chamber, at a distance of 20 cm from the SDBD. The same distance was maintained between the SDBD and the samples during treatments. The beam was then collected in a 500 mm spectrometer (Acton SP2500i, Princeton Instruments) and spectrally resolved in the UV, VIS and near infrared (NIR) regions. OAS acquisitions were performed using a grating with a resolution of 150 mm-1 and setting a width of 10 µm for the inlet slit of the spectrometer. A photomultiplier tube (PMT-Princeton Instruments PD439) connected to a fast oscilloscope (Tektronix MSO46) was used as detector to allow fast acquisitions (time resolution of 40 ms). The PMT amplification factor was kept constant for all acquisitions. Prior to every measurement, the plasma chamber was opened and flushed with air for 5 minutes to ensure identical initial conditions. Each measurement was repeated 3 times.

2.5. Effect of CAP on natural contaminated sundried tomatoes

To evaluate fungal inhibition, the most contaminated batches were subjected to decontamination. For each batch, ten different tomatoes were subjected to the CAP-NOx treatment (5, 10, 20, 30, min) and successively treated as described in paragraph 2.2.1.

2.6. Effect of CAP on spore germination

For the most frequent species found in the control samples of sundried tomatoes, the *in vitro* resistance/sensibility to CAP-NOx exposure time was determined. For this purpose, the spores of *A. niger* PSJ38, *A. tubingensis* PSJ100, *A. flavus* PSJ30, *Aspergillus chevalieri* PSJ144 and *Alternaria alternata* PSJ77 were collected according to the method described by Molina-Hernandez et al. (2022), standardized at a wavelength of 620 nm to obtain an optical density (OD) of 0.1 AU, which corresponds to 1.0×10^5 spores/mL. The different spore suspensions were placed on petri dishes and treated with CAP for 5, 10, 20, 30, 40 and 50 min, respectively. After the treatment, an aliquot of 20µL of the spore suspension was inoculated into glass slides with a thin layer of MEA and incubated at 30 °C for 16 h. Untreated spores were considered as controls. Then, spore germination was observed with a light microscope. Spores were considered germinated when their germ tube was longer than that of the same spore (Peralta-Ruiz et al., 2020). All the experiments were performed in triplicate, and a total of 200 spores were counted for each sample.

2.7. Assay of cell surface hydrophobicity

The hydrophobicity index of the outermost surface of the spores was determined by microbial adhesion to hydrocarbons, according to the methodology reported by Wang et al. (2017). The spore suspension solutions were washed twice and then resuspended in PBS to an OD600=1. The absorbance of the spore suspension was measured and defined as A1. Subsequently, one milliliter of n-butyl alcohol was then added to 1 ml of the cell suspension in a 15-ml falcon tube. After vortexing for 30 s and 3 minutes of incubation, separation occurred. The absorbance of the lower aqueous phase was defined as A2. Hydrophobicity is then expressed as percentage calculated using the following equation:

$$\text{Hydrophobicity (\%)} = (A1 - A2)/A1.$$

2.7. Spore viability

To analyze spore viability immediately after CAP treatment, the spores most frequently found in sundried tomatoes were stained with a mixture of CFDA (carboxyfluorescein diacetate) and propidium iodide (PI) according to methodology reported by Molina-Hernandez et al. (2022).

While the green fluorescent dye CFDA is able to penetrate both intact and damaged cell membranes, the red fluorescent dye PI can only penetrate cells with a significant membrane damage (Molina-Hernandez et al., 2021). 10^4 spore suspension in PBS was treated with CAP-NOx for 5, 10, 20, 30 and 40 min, then stained with both dyes. A Nikon A1R confocal imaging system (Nikon Corp., Tokyo, Japan) was used to observe spore viability.

2.8. Texture analysis of the sundried tomatoes

Firmness (F), skin strength (SS) and elasticity (E) of control and treated tomato samples were evaluated using a texture analyzer (TA.HDi 500; Stable Micro Systems, Godalming, UK) according to the method described by Serhat Turgut et al. (2018). Briefly, a Perspex blade (A/LKB) was used for F measurements of tomato samples at the speed of 2 mm/s. For each tomato, two measurements were made. SS and E were determined using a 2-mm cylindrical stainless probe at the speed of 1 mm/s. For each tomato, 3 points were punctured. For each sample, three tomato slices were measured. F and SS were expressed in g. E was expressed in mm.

Statistical analyses

For the *in vitro* studies, to evaluate both the CAP effect on fungal spore germination and the reduction in fungal mycelial growth in response to the treatments, data from each sampling point were shown as the mean ± SD and statistically analyzed by ANOVA, followed by individual comparisons using Duncan's Multiple Range Test, at $p \leq 0.05$ and using Pearson correlation as a measure of linear association between treatments.

To describe the kinetics of spore inactivation due to time of CAP-NOx treatment, the reparametrized Weibull model proposed by De Flaviis & Sacchetti (2022), in the form of a survival function, was fitted. The model was reformulated as follows:

$$F(t) = N_0 \left\{ e^{\left[-\left(\frac{t}{\beta}\right)^{\frac{e\beta\mu_\beta}{N_0}} \right]} \right\} \qquad (1)$$

The Weibull model, extensively used in many applications (e.g., analysis of non-linear survival curves), was chosen because it can fit different shapes of decay (e.g., sigmoidal curves, long-tailed curves, first order decay) and is a very simple and flexible model (van Boekel, 2008). Moreover,

the reparametrized Weibull model utilized in this study allows to obtain three meaningful parameters for the interpretation of the kinetics of spore inactivation: i) the initial percentage of germination (N_0); ii) the failure time (β), corresponding to the CAP-NOx treatment time when 63.2% of the kinetics are reached; iii) the reduction rate at the failure time (μ_β). The least squares criterion and the "Levenberg–Marquadt" method were used to fit the models and estimate the parameters N0, β and μ_β. The goodness of fit of the models was evaluated considering the R^2, the coefficient of variation of the root means square error (CV(RMSE)) and the Akaike's Information Criterion (AIC). Moreover, the maximum reduction rate (μ_{max}) and the lag phase (λ), corresponding to the so-called "shoulder effect" were calculated following the equations reported by De Flaviis & Sacchetti (2022):

$$\mu_{max} = \mu_\beta e \left(\frac{D}{e}\right)^D \quad (2)$$

$$\lambda = \beta[D^{-D} - (D^{-D} - D^{1-D})(e^D)] \quad (3)$$

Where *D* is:

$$D = \frac{\mu_\beta e\beta - N_0}{\mu_\beta e\beta} \quad (4)$$

Statistical differences of estimated and calculated parameters among fungal spores were analyzed by one-way ANOVA and Least Significant Difference (LSD) post-hoc test. Non-linear regressions were performed using Wolfram Mathematica software (Wolfram Research, Inc.).

3. Results

3.1 Cold Atmospheric Plasma (CAP)

The temporal evolution of O_3 and NO_2 was monitored using OAS. Coherently with the high SPD involved in the treatments, no O_3 was detected, whereas a significant NO_2 concentration was measured and was observed to increase with time, as shown in Figure 1.

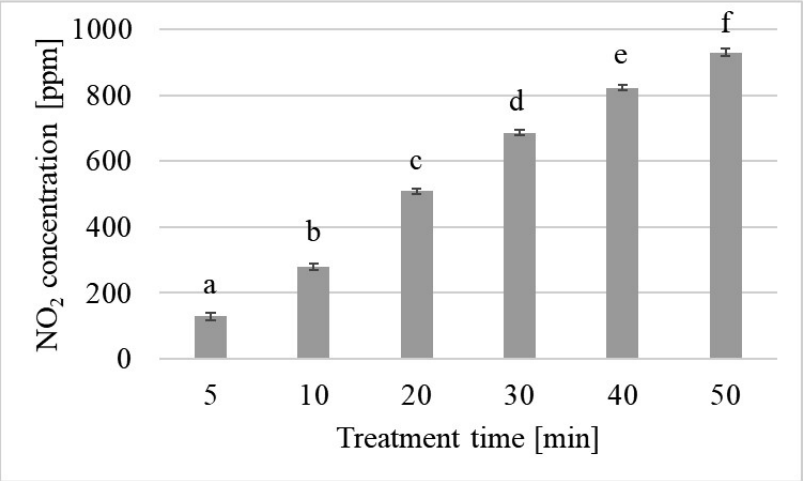

Figure 1. Values of NO_2 after different treatment times. The values are the mean of three repetitions. In each panel, data are mean ± SD, and statistical significance is specified with letters (*$p \leq 0.05$ as determined by paired Student t-test).

3.2 Fungal contamination in sundried tomatoes

In this study, sundried tomatoes samples were tested for the presence and levels of filamentous fungi contaminants. The analysis revealed that all the tomatoes samples were contaminated with spores that germinated and produced proliferous mycelia, although with high variability in the fungal incidence.

A total of 220 filamentous fungi were isolated, and 78, representative of all the sundried tomatoes samples, were identified morphologically at a genus level and successively identified at a species level by PCR. The isolates belonged to 20 genera and represented a total of 32 different species (Table S1). Among the fungal species recovered, *Psathyrella candolleana* and *Trametes elegans* belonged to Basidiomycetes and the other species belonged to Ascomycetes. The relative abundance of the species identified showed that the genus *Aspergillus* supported 47% (94 isolates) of the cultivatable mycobiota, followed by *Alternaria* (6.8%), *Stemphylium* (6.41%), *Chaetomium* (8.1 %), *Arthrinium* (4.1%), and *Penicillium* (3.6 %). Other fungal genera such as *Rhizopus, Eutypella, Chrysonilia, Byssochlamis, Psathyrella, Trimmatothelopsis, Canariomyces, Corynoascus, Trametes, Eutypella, Amesia, Aporospora, Ovatospora, Cladosporium, Gymnascella* were also present at lower levels ranging from 1.8 % to 2.7 %.

As shown in Figure 2, the most frequent and abundant species in sundried tomatoes were *Aspergillus niger* and *Aspergillus tubingensis,* which were present in 6 and 4 out of 24 samples,

representing respectively 9.1 % and 7.3 % of all isolated strains, followed by *Aspergillus chevalieri* (5.9 %), *Aspergillus flavus* (5.9%)*, Alternaria alternata* (5.9 %), and *Aspergillus fumigatus* (4.5%). The other species were isolated less frequently, and their abundance was very low. It should be highlighted that some batches showed very low fungal incidence, consisting of single species and in particular of A. *chevalieri, A. fumigatus, A. alternata, P. citrinum, A. nidulans, A. cristatus, Eutypella microtheca, and Crysonilia sitophyla* (batches 1, 5, 6, 9, 12, 13, 14, 19, 21, and 23, respectively). The batches with low fungal incidence were probably added with high salt concentration during production.

3.3. Effect of CAP-NOx treatments on the spores naturally present in sundried tomatoes

Different exposure times to CAP-NOx were tested to achieve the highest fungal inactivation on the tomatoes surface. In detail, for the most contaminated batches (4, 7, 8 and 20), ten randomly selected tomato samples were exposed to CAP-NOx for 5, 10, 20 and 30 min. Our results showed a higher fungal inactivation by CAP treatment on the smooth surface of tomatoes than on the inner face (data not shown), probably due to the lower accessibility of the CAP-NOx species to spores adhering to the rough surfaces of the sundried tomatoes. Some of the fungal species isolated from the control samples were rapidly inactivated and reached undetectable levels after only 10 min of CAP-NOx. For example, in batch 7, we isolated *A. flavus, A. chevelieri, A. alternata, A. niger, A. tubingensis, Eutypella microtheca, Amesia cymbiformis,* but after 5 min of treatment *Eutypella microtheca, Amesia cymbiformis, A. chevalalieri* and *A. tubingensis* were no longer found. With the increase of exposure time to 10 min, we isolated only *A. alternata, A. flavus* and *A. niger* and after 30 minutes of treatment, *A. niger* was the only isolated species under artificial environmental conditions (95 % HR and 26°C) with a lower incidence than in the control samples. Thus, 30 mins of exposure to CAP-NOx was able to reduce fungal contamination by 76.5 %.

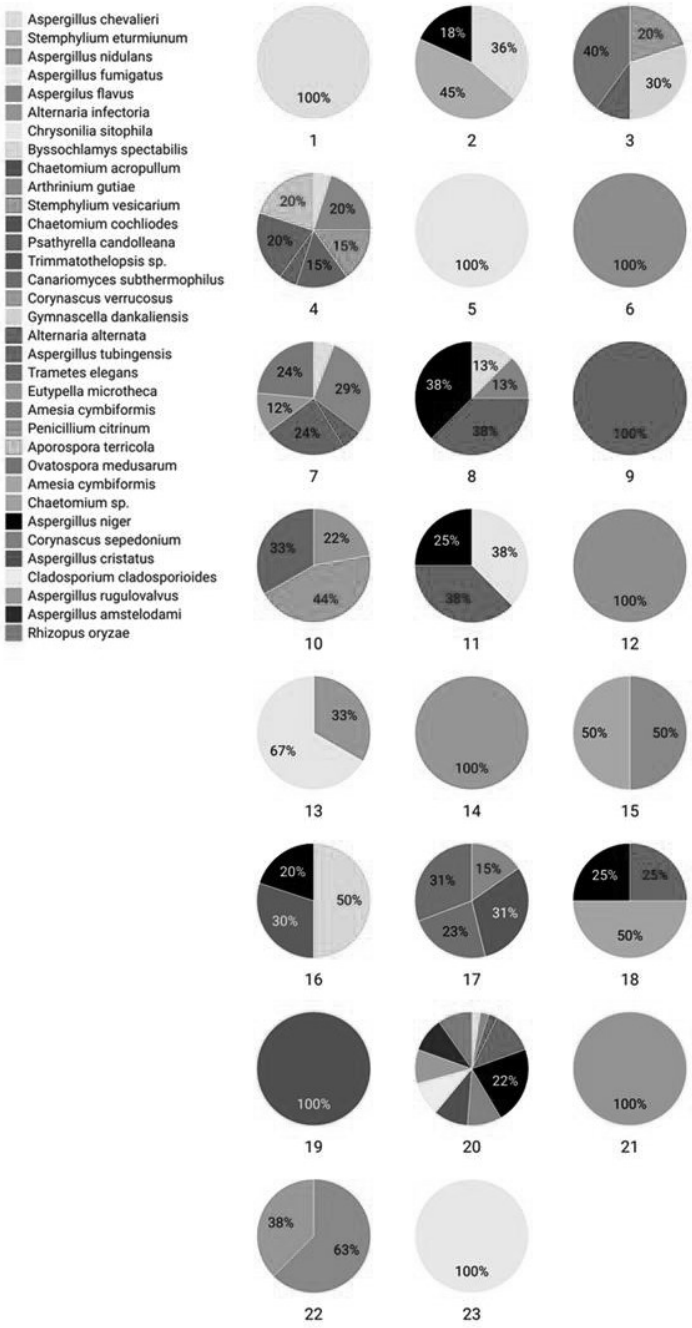

Figure 2. Frequency of the filamentous fungi isolated on the surface of sundried tomatoes belonging to different batches. Created with Datawrapper.

3.4. Effect of CAP-NOx time exposure on spore germination

To investigate the inactivation dynamics of CAP-NOx on spore germination *in vitro*, we considered the spores of selected strains of the species most commonly isolated in the tomatoes batches such as *A. alternata* PSJ77 *A. chevalieri* PSJ144, *A. tubingensis* PSJ100, *A. flavus* PSJ30, and *A. niger* PSJ38. In general, the CAP-NOx treatments significantly reduced spore germination but with different exposure times. In fact, spores of *A. chevalieri PSJ144* showed a greater reduction (almost 90%) immediately after 5 minutes of CAP treatment. Increasing the exposure time up to 30 minutes, a strong reduction ($p \leq 0.05$) of spore germination was observed in *A. alternata* PSJ77 and *A. tubingensis PSJ100* (98 and 92%, respectively). However, spores of *A. niger* PSJ38 and *A. flavus* PSJ30 showed the lowest percentage of non-germinated spores in the same treatment. For these two species, the exposure time was extended to 50 min, and the inhibition of spore germination of *A. niger* PSJ38 and *A. flavus* PSJ30 was achieved at 98 and 95%, respectively, after 40 minutes of CAP-NOx treatment, thus indicating a major resistance of these two species to CAP-NOx treatments.

To study the spore inactivation dynamics, the reparameterized Weibull function was modeled to provide useful species-specific information on germination kinetics as a function of time of CAP-NOx treatment. The regressions are shown in Figure 3 and individually plots in figure S1, while their parameters and goodness-of-fit indexes were listed in Table 3. The parameter β proved to be an interesting indicator of spore resistance as it indicates the time required to reduce the initial value (N_0) to the 63.2%. In this regard, *A. flavus* and *A. niger* showed the highest β time, followed by *A. tubigensis* and *A. alternata*. *A. chevalieri* was the most sensitive spore, since β was reached after only 0.1 minutes of treatment. Generally, μ_β and μ_{max} confirmed this trend, showing the highest reduction rates in *A. chevalieri* that resulted the spore inactivated faster by the treatment. It is noteworthy that although *A. alternata* showed a relatively low failure time (β), it was also characterized by the lowest reduction rates. Concerning the goodness of fit, the models fitted considerably well as shown by the CV(RMSD) in Table 2, except for *A. alternata* that fitted slightly worse.

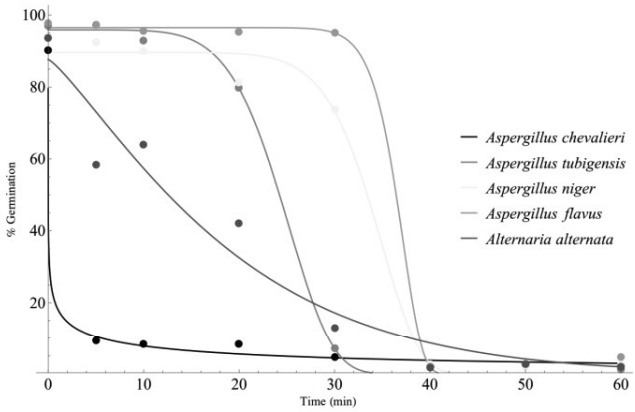

Figure 3. Kinetics of germination reduction in five different fungal spores, as a function of time of treatment, fitted by the Weibull reparametrized model. Dots indicate real data as means of three replications. The regression parameters were listed in Table 3.

Table 3. Estimated and calculated parameters from germination kinetics. Different letters in the same column indicate significant differences ($p < 0.05$) according to LSD post-hoc test. Goodness of fit indexes were reported as mean ± standard deviation.

	Estimated parameters[1]			Calculated parameters[2]		Goodness of fit		
	N_0 (%)	μ_β (%/min)	β (min)	μ_{max} (%/min)	λ (min)	R^2	CV(RMSD)	AIC
Aspergillus flavus	96.5^{a}	17.8^{ab}	37.2^{a}	17.9^{a}	33.8^{a}	0.999 ± 0.000	3.38 ± 0.15	43.09 ± 0.82
Aspergillus niger	89.6^{b}	9.2^{ab}	35.3^{b}	9.2^{b}	29.2^{b}	0.997 ± 0.000	6.55 ± 0.33	51.91 ± 0.54
Aspergillus tubigensis	95.9^{a}	8.9^{ab}	25.9^{c}	9.0^{b}	19.1^{c}	0.999 ± 0.000	3.74 ± 0.40	40.59 ± 1.75
Alternaria alternata	87.5^{b}	2.0^{b}	20.2^{d}	3.3^{c}	0.7^{d}	0.975 ± 0.003	21.91 ± 1.25	63.88 ± 0.39
Aspergillus chevalieri	90.3^{b}	152.1^{a}	0.1^{e}	$\rightarrow\infty$[3]	0[3]	0.998 ± 0.000	8.65 ± 1.01	36.59 ± 1.84

[1] Computed by fitting Eq. 1.
[2] Computed by using Eq. 2 and 3.
[3] Values theoretically assigned, as it is impossible to calculate these parameters when no inflection point is present.

3.5. Changes in spore morphology

Microscopical analyses revealed differences in cell morphology as shown in Figure 4. In this case, a clear loss of spore integrity was observed after only 5 and 30 minutes of CAP-NOx for the spores of *A. chevalieri* PSJ144 and *A. tubingensis* PSJ100, respectively. Intense bombardment with NOx radicals in *A. chevalieri* PSJ144 and *A. alternata* PSJ77 caused serious lesions on the spore surface,

where the spores appeared perforated. The loss of pigmentation of the spores of *A. niger* PSJ38 with increasing exposure time was very interesting, with the color changing from classical black to pale yellow, while in the spores of *A. flavus* PSJ30 the color changed from yellow-green to white. In addition, the spore surface appeared very smooth and homogeneous after CAP-NOx treatment.

To determine if phenotypic changes were correlated with spore viability, fungal spores subjected to CAP-NOx treatment were examined for viability, using CFDA and PI. Live spores stained green and dead spores stained both red (Fig 5). Membrane permeability detection showed that almost all the spores treated with CAP-NOx were stained red after 30 minutes or longer, suggesting that the cell membrane was unable to maintain its function, which could lead to cell death. These observations were reinforced by the lack of viability in extended CAP-NOx treatment.

As observed, the spores of *A. chevalieri* PSJ144 exhibited a cell membrane damage after 5 min of treatment, which reduced their viability by 96.77%, while the spores of *A. tubingensis* PSJ100 and *A. alternata* PSJ77 required more time (30 min) to reach similar values (94.59 and 97.22 respectively). In contrast, the spores of *A. niger* PSJ38 and *A. flavus* PSJ30 were strongly resistant, as they required 40 mins treatment to show a loss of viability of 93.33 and 94.12%, respectively.

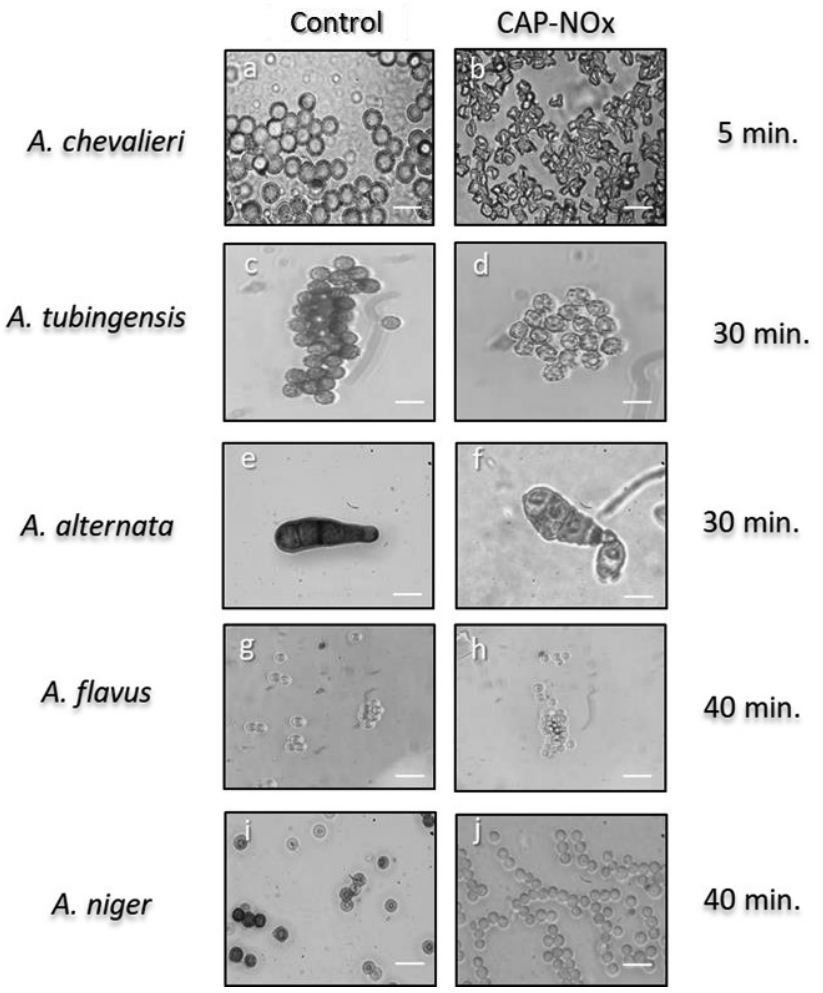

Figure 4. Microscopic visualization of *A. chevalieri* PSJ144, *A. tubingensis* PSJ100*, A. alternata* PSJ77*, A. flavus* PSJ30 and *A. niger* PSJ38 spores before and after treatment with CAP-NOx. Scale bars, 10 µm.

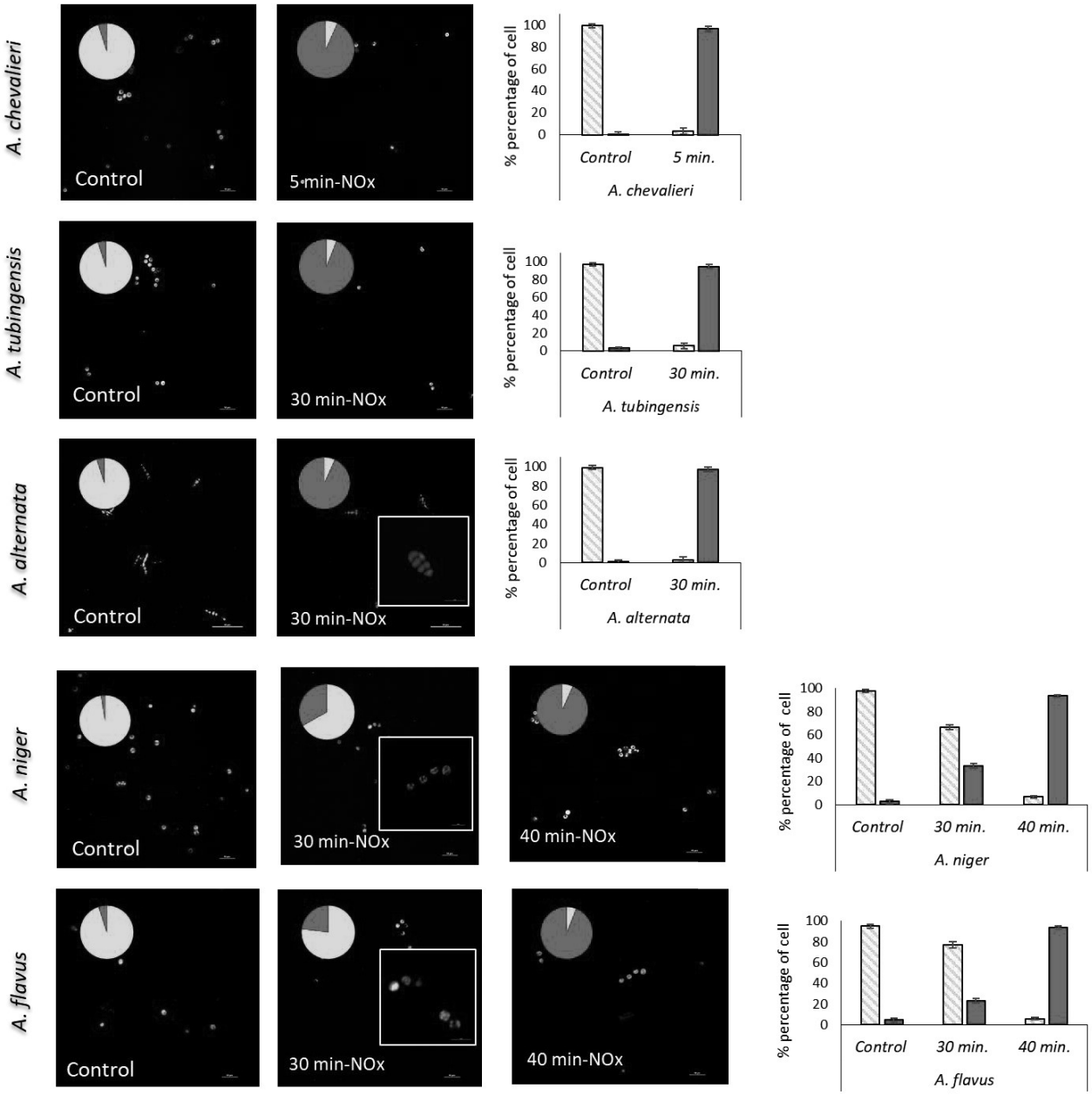

Figure 5. Confocal laser scanning microscopy analysis of cell viability in *A. chevalieri* PSJ144, *A. tubingensis* PSJ100*, A. alternata* PSJ77*, A. flavus* PSJ30, and *A. niger* PSJ 38 after treatment with CAP-NOx. Cells were stained with green fluorescence CFDA (carboxyfluorescein diacetate) and red propidium iodide (PI) dyes. Bars indicate the percentage of cell live (green) and death (red) spore. Image zoom of spores indicate a total loss of viability after treatment with CAP-NOx. Scale bar 10 um.

3.6. Changes in spore hydrophobicity

Hojnik et al. (2019) suggested that the resistance of *A. flavus* to direct exposure to gaseous plasma is due to the surface properties of *Aspergillus* spp. spores, which have extremely hydrophobic properties. For this reason, we measured this property in the spores of the species studied here. As can be seen in Figure 6, the most resistant strains to CAP-NOx treatments, namely *A. niger* PSJ38 and *A. flavus* PSJ30, had the highest hydrophobicity index compared to the most sensitive strains *A. chevalieri* PSJ144, *A. tubingensis* PSJ100, *and A. alternata* PSJ77. Statistical analysis using Pearson correlation showed a high correlation (p=0.98) between hydrophobicity and resistance to CAP-NOx. It is should be emphasized that hydrophobicity was significantly reduced in all strains after only 5 min of exposure; however, in the most resistant strain (*A. niger* PSJ38), exposure to CAP-NOx promoted a gradual change from the hydrophobic to the hydrophilic state of the spore surface.

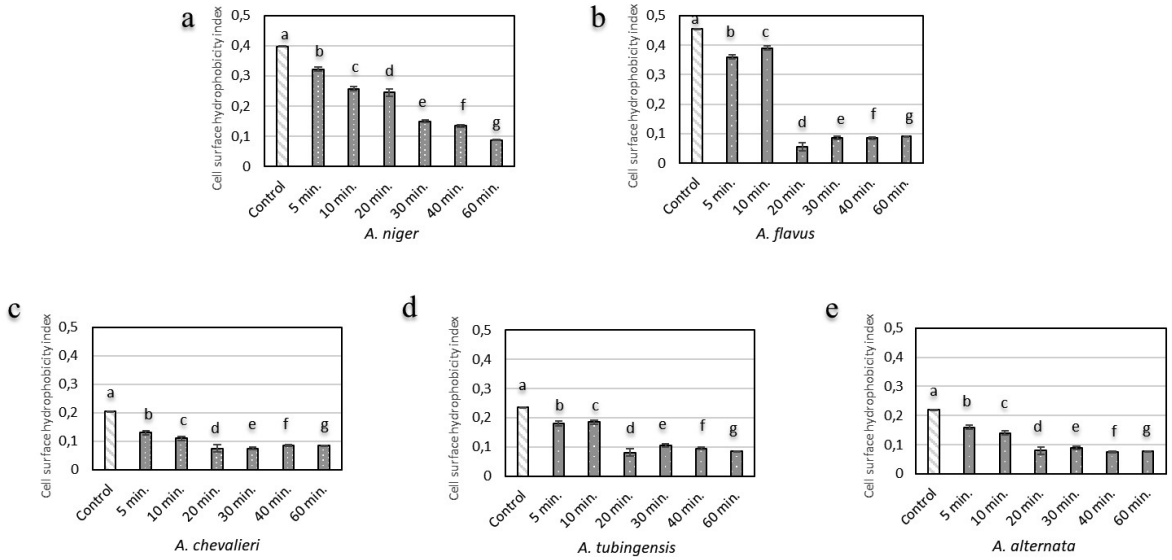

Figure 6. Analysis of the surface hydrophobicity of the *A. niger* PSJ38 (a); *A. flavus* PSJ30 (b); *A. chevalieri* PSJ144(c); *A. tubingensis* PSJ100(d), and *A. alternata* PSJ77(e) after treatment with CAP-NOx. Data were obtained from three independent experiments. Different letters represent significant differences among the sample ($p < 0.05$; Tukey HSD post-hoc test).

3.7. *Effect on the texture of the sundried tomatoes*

Table 4 shows the texture parameters measured in sundried tomatoes after different exposure times. After an exposure time of 5 min, no significant differences were observed in the parameters considered. On the contrary, with increasing treatment times over 10 min, some changes were observed. Compared with the untreated sample, firmness was higher after 10 min but lower after 20 and 30 min. Skin Strength decreased after 20 min, but increased after 30 min. Elasticity was unchanged until the 20 min treatment, and then increased after 30 min.

Table 4. Textural values in sundried tomatoes untreated and treated with CAP treatments.

Property	Control	5 min.	10 min.	20 min.	30 min.
Firmness	483.3±133.1[a]	426.0±104.9[a]	606.6±124.8[b]	252.5±139.8[c]	426.0±104.9[c]
Skin Strength	1325.8±460.7[a]	1307.3±202.3[a]	1319.0±353.5[a]	823.4±521.5[b]	1697.5±161.4[c]
Elasticity	5.7±2.7[a]	6.5±1.0[a]	6.5±1.6[a]	6.1±2[a]	7.6±1.8[b]

[a,b,c] Means in the same row with different superscripts are significantly different (P 0.05).

Discussion

Fungal decontamination is one of the biggest challenges for the food industry during production. Some fungal species cause a wide range of diseases affecting numerous economically important host plants, including tomatoes, cereals, potatoes, cabbage, broccoli, carrots, ornamentals, citrus fruits, and apples (Kokaeva et al., 2018). Moreover, fungal contamination occurs not only at harvest or post-harvest, but also during processing. In this context, tomatoes (*Solanum Lycopersicum* L.) are processed into a variety of products such as dried tomatoes, where drying is a critical processing step that can lead to contamination by fungi from the environment, which can affect the quality of the product (Zansani et al., 2019). In fact, the importance of fungal contamination in food products refers not only to the possible degradation activity, but also to the ability of many of them to produce mycotoxins. In this study, we investigated the diversity and occurrence of fungal species in sundried tomatoes from the market, and for the first time, the efficacy of the CAP-NOx regime on the decontamination of fungal spores.

As our results from 24 different batches showed, the most frequently occurring fungal genus found in sundried tomatoes was *Aspergillus* (47.4%). This result is in agreement with Kalyoncu et al. (2005), who described this genus as one of the most important genera isolated in tomatoes and

516 tomato paste. The consequence of the presence of *Aspergillus* is the possible contamination with
517 mycotoxins, of which the most important are aflatoxins (B_1, B_2, G_1, G_2), ochratoxin A, and, at to
518 a lesser extent, fumonisins. In different studies, the presence of fungal species potentially
519 producing mycotoxins such as *A. flavus* (aflatoxin, sterigmatotistin) *A. fumigatus* (fumitremorgin),
520 *A. niger* and *A. tubingensis* (ochratoxin A) was detected in tomatoes, tomato paste, and sundried
521 tomatoes (Han et al., 2019; Kalyoncu et al., 2005; Kokaeva et al., 2018; Sanzani et al., 2019).
522 Other genera that showed high frequency in our batches were *Alternaria* (6.8%) and *Chaetomium*
523 (6.3%). The genus *Alternaria* (*A. alternata* and *A. infectoria*), which were present in a significant
524 number of samples (62%), are capable of producing a large number of toxins, including alternariol,
525 alternariol monomethylether, altenuene, tenoxin and tenuazonic acid. *A. alternata* is a saprophytic
526 pathogen of tomato, a necrotrophic latent fungus that causes black spots on the surface of ripening
527 tomatoes, resulting in frequent postharvest losses (Encinas-Basurto et al., 2017). On the other
528 hand, *Chaetomium* with the species *Chaetomium cochliodes* and *Chaetomium acropollum*, are
529 globally ubiquitous fungi found in soil and degraded cellulosic materials (Salo et al., 2020).
530 The presence of potentially mycotoxigenic fungi in sundried tomatoes makes it important to adopt
531 systems for disinfection and to minimize their impact on the quality of the treated product. Our
532 results demonstrate that CAP-NOx regime can be a promising strategy to decontaminate the
533 surface of sundried tomatoes from fungal spores. In fact, the reactive species generated by CAP
534 under NOx regime compromise to a great extent the integrity of cells (Misra et al., 2011). In our
535 study, the NOx regime was achieved by applying a sufficiently high surface power density to the
536 plasma discharge. Indeed, NOx production with cold atmospheric plasmas in air is known to be a
537 threshold process guided by the SPD by controlling the excitation and dissociation of N_2 molecules
538 (Simoncelli et al., 2019). Once these molecules are sufficiently excited, their reaction with O_2 and
539 O_3 molecules leads to the formation of a complex NOx chemistry, including NO, N, NO_2, NO_3,
540 N_2O_5 (Hojnik et al., 2019; Molina-Hernandez et al., 2022).
541 Although the antifungal activity of CAP-O_3 has been demonstrated by several authors (Ambrico
542 et al., 2020; Kang et al., 2014; Molina-Hernandez et al., 2022; Panngom et al., 2014), studies on
543 the antifungal activity of CAP-NOx are lacking. Our data support the hypothesis that exposure of
544 tomatoes to CAP-NOx may be associated with the decontamination of fungal spores on the surface
545 of sundried tomatoes, which depends on the CAP-NOx exposure time, and the characteristics of
546 the target fungi. The results of our *in-situ* study pointed out the efficacy of the treatment in terms

of spore inactivation in naturally contaminated tomatoes, which increased with increasing exposure time to CAP-NOx. In fact, we observed a reduction of fungal contamination of 76.5 % after 30 mins of exposure to CAP-NOx. In this regard, the spores of *A. flavus* PSJ30 and *A. niger* PSJ38 were the most resistant after 30 min treatment, resulting in a high survival of these fungi compared to other fungal species found in the tomatoes batches here analyzed. These results indicate that the increased levels of reactive nitrogen species (RNS) following plasma treatment likely played a role in spore inactivation.

The antifungal effect of NO has been previously reported (Weller et al., 2001). However, the comparison of the efficacy of the CAP treatment with previous studies is very difficult because it depends on the generator device, voltage, exposure time, initial microbial density, process gas, working distance, and plasma exposure. Wang et al. (2022) reported 96.84% loss of cell viability and membrane integrity of *Fusarium* spp. after 3-min of CAP using a dielectric barrier surface micro-discharge (SMD) plasma generator. Jo et al. (2014) observed 92% fungal colony forming units (CFU) inhibition of G *Gibberella fujikuroi* on the rice seed surface, after 120 s of exposure. Our results are in agreement with those obtained by Ambrico et al. (2020), who reported that the inactivation of the fungal growth is species dependent. In fact, they observed different survival rates of spores belonging from different fungal species (*Botrytis cinerea, Monilinia fructicola, Aspergillus carbonarius* and *Alternaria alternata)* exposed to SDBD plasma. It is important to highlight that inhibition of spore germination, reduction of viability and morphological alterations of cell surface up to spore destruction of these species, demanded diverse treatment times. Moreover, Pańka et al. (2022) found diverse efficacy of Cold plasma (DBD) treatments on different fungal spores present in seeds, by using 400 W power and 15 s of exposure time. In this case, the treatment was very effective against *Alternaria, Aspergillus, Colletotrichum, Fusarium, Penicillium* genera, being *Aspergillus ochraceus* the most resistant species. For more intense direct DBD systems, a notable study using an air direct DBD on agar plates achieved significant reductions against fungi (1.7 and 1.0 log CFU reductions of *Aspergillus oryzae* and *Alternaria* conidia, respectively, within 10 min) (Julák et al., 2018).

In our study, the specific effect of CAP-NOx treatment on fungal spores was confirmed *in vitro*, demonstrating that the spores of the species studied here were resistant to CAP-NOx in the following order: *A. chevalieri* PSJ144 < *A. alternata* PSJ77 < *A. tubingensis* PSJ100 < *A. flavus* PSJ30 < *A. niger* PSJ38. Interestingly, although *A. alternata* showed a relatively low failure time

(β), it was also characterized by the lowest rates, suggesting that a small group of cell spores could survive a longer treatment time. This may be because *Alternaria* spp. is the only multicellular conidia studied in this work, characterized by a primary cell wall that is melanized and a secondary wall that is not melanized (Ambrico et al., 2020), which may have resulted in a different response to CAP-NOx treatment.

Fungal spore survival in the harsh environment of plasma treatment generally depends on: 1) the spore cell wall, which helps prevent radiation damage to DNA, 2) the type of gas used and the gas flow rate, 3) the relative humidity, and 4) the substrate. Fungal spores are very dense and compact structures surrounded by different layers. In particular, the outer layer of most asexual fungal spores is composed of polysaccharides (chitin and combination of a-glucans and b-glucans), and is surrounded by a rodlet layer with a complex structure composed of a phenolic compound (melanin) and a hydrophobic protein (hydrophin) (El Enshasy, 2022). These compounds form a well-structured monolayer in which a combination of neutral, hydrophilic and hydrophobic amino acids are present and which exhibits a uniform hydrophobicity on the outside of the cell (Moonjely et al., 2018; Wu et al., 2017). Ambrico et al. (2020) observed that RNS have a direct effect on cells, and especially on the outermost layer, the polysaccharide-rich wall. Other authors suggested that the radicals produced during CAP may oxidize the protein of the spore envelope, leading to a loss of the envelope integrity and therefore making the spore more vulnerable to attack by the radicals generated by plasma (Devi et al., 2017). In fact, bombardment with reactive plasma species creates active sites on the surface of the protein, and the RNS introduced by plasma into the protein structure can also act as quenchers (Bußler et al., 2015). In addition, the accumulation of charged particles on the surface of spores and electrostatic forces can lead to rupture of the cell membrane and subsequently cause cell death (Laroussi et al., 2003; Mendis et al., 2000). In a study conducted by Hojnik et al. (2019) on spores of *A. flavus* treated with both direct gaseous plasma treatment and indirect treatment with plasma activated aqueous broth (PAB), it was found that direct treatment was more effective than PAB, and this result was attributed to the hydrophobic surface properties of the spores, which make them much more resistant to RONS in the liquid phase. Herein, we found that the survival of spores of the 5 different strains studied to CAP-NOx was highly dependent on spore hydrophobicity. In fact, the spores of *A. niger* PSJ38 and *A. flavus* PSJ30, which turned out to be the most hydrophobic ones, were also more resistant to plasma treatments than *A. chevalieri* PSJ144 spores, which were less hydrophobic. In this respect, spore

hydrophobicity might have contributed to the spore resistance, due to the lower interaction between NOx radicals and the small secreted amphipathic proteins called hydrophobins, which can self-assemble into a monolayer that exhibits a uniform hydrophobicity on the cell exterior (Moonjely et al., 2018). In particular, the amino acids that form the hydrophobins of *A. chevalieri* PSJ144 might be more polar and therefore more easily targeted by radical species than less polar ones. In addition, it is important to underline that after each CAP-NOx treatment the spores lost their hydrophobicity, which suggests a direct or an indirect effect of CAP on the protein architecture of the cell wall, leading to a reduction in cell vitality. The degradation of cellular proteins by CAP is poorly described in literature and should be investigated.

Another aspect to consider in spore resistance to CAP-NOx is the presence of melanin, a pigment known to contribute to the rigidity of spore cell walls, protecting the cell from stressors such as temperature, UV-radiation, and reactive oxygen species (Ott et al., 2021). In this respect, our data support the observations of Ambrico et al. (2020), who found that the darkest-colored spores of *A. carbonarius* and *A. Alternaria* showed higher resistance to the treatment compared to the lighter pigmented and thinner walled spores of *B. cinerea* and *M. fructicola*. In fact, in our study the spores of *A. niger* PSJ38 and *A. alternata* PSJ77 were more resistant to CAP-NOx than those of *A. chevalieri* PSJ144, which showed a 98% inactivation after 5 min of plasma exposure. It should be emphasized that melanin pigments quench reactive oxygen and nitrogen species, and therefore spores depleted of this pigment are more susceptible to ROS and RNS (Ott et al., 2021). This may be the case for *A. niger* PSJ38, which was depigmented after 40 min of treatment and showed an increasing percentage of spore inactivation. Pal et al. (2014) also found that loss of melanin was associated with increased susceptibility of *Aspergillus* spp. to damage by reactive oxygen species. Therefore, we can hypothesize that proteins of the wall are one of the first targets for biologically active agents generated by CAP-NOx, and that the efficacy of plasma in spore inactivation depends not only on spore hydrophobicity, but also on the presence of melanin that could mitigate the effects of CAP-NOx on spore survival.

Textural properties are important characteristics that determine the product quality, as they strongly influence consumer's perception. The observed changes in the considered parameters occurred after 10 min of treatment but did not show a clear trend with respect to treatment duration. The texture of sun-dried tomatoes is very complex, and, to our knowledge, there are no reports on the effects of CAP on the structural properties of these products, so it is very difficult to draw

conclusions. To understand whether the observed changes cause significant effects on dried tomato quality, the texture should probably be evaluated by a panel test.

Compared with other methods for reducing fungal growth, CAP-NOx is a fast technology that can decontaminate foods and does not leave toxic residues or post-processing exhaust gases. In addition, it represents a non-thermal alternative for food decontamination, which can be considered appealing in view of the recent rise of energy prices. Moreover, this method is certainly sustainable, because it avoids the impact of chemicals on both the product and the environment. Thus, CAP-NOx could be an attractive approach for producing high-quality tomato products with an extended the shelf-life, with interesting potential effects on the market, considering the possibility to enlarge the trade, differentiate the range of commercialized products, reduce the waste and the cost of the discharge, with economic and social advantages. Furthermore, post-harvest treatments with chemicals involve costs for controlling residues, with a direct impact on the price of the finished product (Hernández-Torres et al., 2022).

CONCLUSIONS

This study is a first attempt to apply CAP-NOx for treating a dried fruit. The results presented in this paper show for the first time the inhibitory activity of CAP-NOx species against the spores of the most frequent species found in sundried tomatoes, and namely *A. alternata, A. chevalieri*, *A. tubingensis*, *A. flavus* and *A. niger*. We demonstrated that CAP treatment can effectively reduce the survival rate (76.5%) of fungi on the surface of sundried tomatoes. The Weibull reparameterized model proposed by De Flaviis & Sacchetti (2022) gave useful information on the species-specific inactivation kinetics after CAP-NOx treatment, which involves a differential germination of the fungal spores associated with sundried tomatoes. Although four of the tested *Aspergillus* species have a similar asexual morphological type, they perform differently under the nitrosative stress induced by CAP-NOx. This behavior may be correlated with spore hydrophobicity, which was major in the most resistant spores as *A. niger*. However, more research needs to be done to better explain the vector of environmental adaptations in *A. niger* against CAP-NOx. In conclusion, the results of this study open up new perspectives on the potential application of CAP-NOx for fungal decontamination of dried foods.

CRediT authorship contribution statement

Junior Bernardo Molina-Hernandez: Conceptualization, Methodology, Software, Validation, Formal analysis, Investigation, Writing – original draft, **Silvia Tappi**: Methodology, Formal analysis, Writing – review & editing; **Matteo Gherardi**: Methodology, Formal analysis, Writing –review & editing**; Riccardo de Flaviis**: Methodology, Data curation, **Jessica Laika**: Investigation, Formal analysis, **Yeimmy Yolima Peralta-Ruiz:** Investigation, review & editing, **Antonello Paparella:** Supervision, Writing – review & editing**: Clemencia Chaves-López**: Conceptualization, Supervision, Writing – original draft, Project administration.

Declaration of Conflict of Interest

The authors declare no conflict of interest

Funding

The present work is part of the research activities developed within the project "PLASMAFOOD—Study and optimization of cold atmospheric plasma treatment for food safety and quality improvement" founded by MIUR—Ministero dell'Istruzione dell'Università e della Ricerca—PRIN: Progetti di Ricerca di Rilevante Interesse Nazionale, Bando 2017.

References

Abdallah, M. F., Audenaert, K., Lust, L., Landschoot, S., Bekaert, B., Haesaert, G., De Boevre, M., & De Saeger, S. (2020). Risk characterization and quantification of mycotoxins and their producing fungi in sugarcane juice: A neglected problem in a widely-consumed traditional beverage. *Food Control*, *108*, 106811. https://doi.org/10.1016/j.foodcont.2019.106811

Aguiló-Aguayo, I., Charles, F., Renard, C. M. G. C., Page, D., & Carlin, F. (2013). *Aguiló-Aguayo et al. 2013.pdf* (pp. 29–36). https://doi.org/10.1016/j.postharvbio.2013.06.011

Ambrico, P. F., Šimek, M., Rotolo, C., Morano, M., Minafra, A., Ambrico, M., Pollastro, S., Gerin, D., Faretra, F., & De Miccolis Angelini, R. M. (2020). Surface Dielectric Barrier Discharge plasma: a suitable measure against fungal plant pathogens. *Scientific Reports*, *10*(1), 1–17. https://doi.org/10.1038/s41598-020-60461-0

Bußler, S., Steins, V., Ehlbeck, J., & Schlüter, O. (2015). Impact of thermal treatment versus cold atmospheric plasma processing on the techno-functional protein properties from Pisum sativum "Salamanca." *Journal of Food Engineering*, *167*, 166–174. https://doi.org/10.1016/j.jfoodeng.2015.05.036

Canakapalli, S. S., Sheng, L., & Wang, L. (2022). Survival of common foodborne pathogens on dates, sundried tomatoes, and dried pluots at refrigerated and ambient temperatures. *Lwt*, *154*, 112632. https://doi.org/10.1016/j.lwt.2021.112632

De Flaviis, R., & Sacchetti, G. (2022). Reparameterization of the Weibull model for practical uses in food science. *Journal of Food Science*, *87*(5), 2096–2111. https://doi.org/10.1111/1750-3841.16124

Delgado-Ospina, J., Acquaticci, L., Molina-Hernandez, J. B., Rantsiou, K., Martuscelli, M., Kamgang-Nzekoue, A. F., Vittori, S., Paparella, A., & Chaves-López, C. (2021). Exploring the capability of yeasts isolated from colombian fermented cocoa beans to form and degrade biogenic amines in a lab-scale model system for cocoa fermentation. *Microorganisms*, *9*(1), 1–17. https://doi.org/10.3390/microorganisms9010028

Devi, Y., Thirumdas, R., Sarangapani, C., Deshmukh, R. R., & Annapure, U. S. (2017). In fl uence of cold plasma on fungal growth and a fl atoxins production on groundnuts. *Food Control*, *77*, 187–191. https://doi.org/10.1016/j.foodcont.2017.02.019

El Enshasy, H. A. (2022). Fungal morphology: a challenge in bioprocess engineering industries

for product development. *Current Opinion in Chemical Engineering*, *35*, 100729. https://doi.org/10.1016/j.coche.2021.100729

Encinas-Basurto, D., Valenzuela-Quintanar, M. I., Sánchez-Estrada, A., Tiznado-Hernández, M. E., Rodríguez-Félix, A., & Troncoso-Rojas, R. (2017). Alterations in volatile metabolites profile of fresh tomatoes in response to Alternaria alternata (Fr.) keissl. 1912 infection. *Chilean Journal of Agricultural Research*, *77*(3), 194–201. https://doi.org/10.4067/S0718-58392017000300194

Glass, N. L., & Donaldson, G. C. (1995). Development of primer sets designed for use with the PCR to amplify conserved genes from filamentous ascomycetes. *Applied and Environmental Microbiology*, *61*(4), 1323–1330. https://doi.org/10.1128/aem.61.4.1323-1330.1995

Gorgüç, A., Gençdag, E., Okuroglu, F., Yılmaz, F. M., Bıyık, H. H., Oztürk ¨ Kose, S., & Ersus, S. (2021). *Single and combined decontamination effects of power-ultrasound, peroxyacetic acid and sodium chloride sanitizing treatments on Escherichia coli, Bacillus cereus and Penicillium expansum inoculated dried figs* (p. 140). https://doi.org/doi.org/10.1016/j.lwt.2020.110844

Gündüz, G. T., & Korkmaz, A. (2019). *Gündüz and Korkmaz et al. 2019.pdf* (p. 115). https://doi.org/10.1016/j.lwt.2019.108451

Hamanaka, R. B., & Chandel, N. S. (2009). Mitochondrial reactive oxygen species regulate hypoxic signaling. *Current Opinion in Cell Biology*, *21*(6), 894–899. https://doi.org/10.1016/j.ceb.2009.08.005

Han, X., Jiang, H., & Li, F. (2019). Dynamic ochratoxin A production by strains of aspergillus niger intended used in food industry of China. *Toxins*, *11*(2). https://doi.org/10.3390/toxins11020122.

Hao, X., Mattson, A. M., Edelblute C. M., Malik, M. A., Heller, L. C., Kolb, J. C. (2014). Nitric Oxide Generation with an Air Operated Non-Thermal Plasma Jet and Associated Microbial Inactivation Mechanisms. Plasma Process. Polymers. 2014, 11, 1044–1056.

Hegazy, E. M. (2017). Mycotoxin and fungal contamination of fresh and dried tomato. *Annual Research and Review in Biology*, *17*(6), 1–9. https://doi.org/10.9734/ARRB/2017/35571

Heperkan, D., Somuncuoglu, S., Karbancioglu-Güler, F., & Mecik, N. (2012). Natural contamination of cyclopiazonic acid in dried figs and co-occurrence of aflatoxin. *Food Control*, *23*(1), 82–86. https://doi.org/10.1016/j.foodcont.2011.06.015

764 Hernández-Torres, C. J., Reyes-Acosta, Y. K., Chávez-González, M. L., Dávila-Medina, M. D.,
765 Verma, D. K., Martínez-Hernández, J. L., Narro-Céspedes, R. I., Aguilar, C. N. (2022).
766 Recent trends and technological development in plasma as an emerging and promising
767 technology for food biosystems. *Saudi Journal of Biological Sciences*, 29 (4),1957-1980,
768 https://doi.org/10.1016/j.sjbs.2021.12.023.
769 Hojnik, N., Modic, M., Tavčar-Kalcher, G., Babič, J., Walsh, J. L., & Cvelbar, U. (2019).
770 Mycotoxin decontamination efficacy of atmospheric pressure air plasma. *Toxins*, *11*(4).
771 https://doi.org/10.3390/toxins11040219.
772 Jo, Y.K., Cho, J.,Tsai, T.C., Staack, D., Kang, M.H., Roh, J.H., Shin, D.B., Cromwell, W., Gross,
773 D. (2014). A non-thermal plasma seed treatment method for management of a seedborne
774 fungal pathogen on rice seed. Crop Science. 54, 796–803.
775 https://doi.org/10.2135/cropsci2013.05.0331
776 Julák, J., Soušková, H., Scholtz, V., Kvasničková, E., Savická, D., & Kříha, V. (2018).
777 Comparison of fungicidal properties of non-thermal plasma produced by corona discharge
778 and dielectric barrier discharge. Folia microbiologica, 63(1), 63–68.
779 https://doi.org/10.1007/s12223-017-0535-6
780 Kakde, U. B., & Kakde, H. U. (2012). Incidence of post-harvest disease and airborne fungal spores
781 in a vegetable market. *Acta Botanica Croatica*, *71*(1), 147–157.
782 https://doi.org/10.2478/v10184-011-0059-0
783 Kalyoncu, F., Tamer, A. U., & Oskay, M. (2005). Determination of fungi Associated with
784 Tomatoes (Lycopersicum esculentrum M.) and Tomato Pastes. *Plant Pathology Journal*,
785 *4*(2), 146–149.
786 Kang, M. H., Hong, Y. J., Attri, P., Sim, G. B., Lee, G. J., Panngom, K., Kwon, G. C., Choi, E.
787 H., Uhm, H. S., & Park, G. (2014). Analysis of the antimicrobial effects of nonthermal plasma
788 on fungal spores in ionic solutions. *Free Radical Biology and Medicine*, *72*, 191–199.
789 https://doi.org/10.1016/j.freeradbiomed.2014.04.023
790 Karaca, H., Velioglu, Y. S., & Nas, S. (2010). Mycotoxins: Contamination of dried fruits and
791 degradation by ozone. *Toxin Reviews*, *29*(2), 51–59.
792 https://doi.org/10.3109/15569543.2010.485714
793 Kokaeva, L. Y., Belosokhov, A. F., Doeva, L. Y., Skolotneva, E. S., & Elansky, S. N. (2018).
794 Distribution of Alternaria species on blighted potato and tomato leaves in Russia. *Journal of*

795 *Plant Diseases and Protection*, *125*(2), 205–212. https://doi.org/10.1007/s41348-017-0135-
796 3
797 Laroussi, M., Mendis, D. A., & Rosenberg, M. (2003). Plasma interaction with microbes. *New*
798 *Journal of Physics*, *5*, 0–10. https://doi.org/10.1088/1367-2630/5/1/341
799 Laurita, R., Gozzi, G., Tappi, S., Capelli, F., Bisag, A., Laghi, G., Gherardi, M., Cellini, B.,
800 Abouelenein, D., Vittori, S., Colombo, V., Rocculi, P., Dalla Rosa, M., & Vannini, L. (2021).
801 Effect of plasma activated water (PAW) on rocket leaves decontamination and nutritional
802 value. *Innovative Food Science and Emerging Technologies*, *73*(August), 102805.
803 https://doi.org/10.1016/j.ifset.2021.102805
804 Lee, G. J., Sim, G. B., Choi, E. H., Kwon, Y. W., Kim, J. Y., Jang, S., & Kim, S. H. (2015). Optical
805 and structural properties of plasma-treated Cordyceps bassiana spores as studied by circular
806 dichroism, absorption, and fluorescence spectroscopy. *Journal of Applied Physics*, *117*(2), 1–
807 13. https://doi.org/10.1063/1.4905194
808 Makhlouf, J., Carvajal-Campos, A., Querin, A., Tadrist, S., Puel, O., Lorber, S., Oswald, I. P.,
809 Hamze, M., Bailly, J. D., & Bailly, S. (2019). Morphologic, molecular and metabolic
810 characterization of Aspergillus section Flavi in spices marketed in Lebanon. *Scientific*
811 *Reports*, *9*(1), 1–11. https://doi.org/10.1038/s41598-019-41704-1
812 Mendis, D. A., Rosenberg, M., & Azam, F. (2000). A note on the possible electrostatic disruption
813 of bacteria. *IEEE Transactions on Plasma Science*, *28*(4), 1304–1306.
814 https://doi.org/10.1109/27.893321
815 Misra, N. N., Tiwari, B. K., Raghavarao, K. S. M. S., & Cullen, P. J. (2011). Nonthermal Plasma
816 Inactivation of Food-Borne Pathogens. *Food Engineering Reviews*, *3*(3–4), 159–170.
817 https://doi.org/10.1007/s12393-011-9041-9
818 Molina-Hernandez, J. B., Aceto, A., Bucciarelli, T., Paludi, D., Valbonetti, L., Zilli, K., Scotti, L.,
819 & Chaves-López, C. (2021). The membrane depolarization and increase intracellular calcium
820 level produced by silver nanoclusters are responsible for bacterial death. *Scientific Reports*,
821 *11*(1), 1–13. https://doi.org/10.1038/s41598-021-00545-7
822 Molina-Hernandez, J. B., Laika, J., Peralta-Ruiz, Y., Palivala, V. K., Tappi, S., Cappelli, F., Ricci,
823 A., Neri, L., & Chaves-López, C. (2022). Influence of Atmospheric Cold Plasma Exposure
824 on Naturally Present Fungal Spores and Physicochemical Characteristics of Sundried
825 Tomatoes (Solanum lycopersicum L.). *Foods*, *11*(2). https://doi.org/10.3390/foods11020210

826 Moonjely, S., Keyhani, N. O., & Bidochka, M. J. (2018). Hydrophobins contribute to root
827 colonization and stress responses in the rhizosphere-competent insect pathogenic fungus
828 Beauveria bassiana. *Microbiology (United Kingdom)*, *164*(4), 517–528.
829 https://doi.org/10.1099/mic.0.000644
830 Mousavi Khaneghah, A., Hashemi Moosavi, M., Oliveira, C. A. F., Vanin, F., & Sant'Ana, A. S.
831 (2020). Electron beam irradiation to reduce the mycotoxin and microbial contaminations of
832 cereal-based products: An overview. *Food and Chemical Toxicology*, *143*(July), 111557.
833 https://doi.org/10.1016/j.fct.2020.111557
834 Munitz, M. S., Garrido, C. E., Gonzalez, H. H. L., Resnik, S. L., Salas, P. M., & Montti, M. I. T.
835 (2013). Mycoflora and Potential Mycotoxin Production of Freshly Harvested Blueberry in
836 Concordia, Entre Ríos Province, Argentina. *International Journal of Fruit Science*, *13*(3),
837 312–325. https://doi.org/10.1080/15538362.2013.748374
838 Oberoi, H. S., Kalra, K. L., Uppal, D. S., & Tyagi, S. K. (2007). Effects of different drying methods
839 of cauliflower waste on drying time, colour retention and glucoamylase production by
840 Aspergillus niger NCIM 1054. *International Journal of Food Science and Technology*, *42*(2),
841 228–234. https://doi.org/10.1111/j.1365-2621.2006.01331.x
842 Ott, L. C., Appleton, H. J., Shi, H., Keener, K., & Mellata, M. (2021). High voltage atmospheric
843 cold plasma treatment inactivates Aspergillus flavus spores and deoxynivalenol toxin. *Food*
844 *Microbiology*, *95*, 103669. https://doi.org/10.1016/j.fm.2020.103669
845 Pańka, D., Jeske M., Łukanowski, A., Baturo-Cieśniewska, A., Prus P., Maitah M., Maitah K.,
846 Malec K., Rymarz D., Muhire JdD., Szwarc K. (2022). Can Cold Plasma Be Used for
847 Boosting Plant Growth and Plant Protection in Sustainable Plant Production? *Agronomy*.
848 12(4):841. https://doi.org/10.3390/agronomy12040841
849 Panngom, K., Lee, S. H., Park, D. H., Sim, G. B., Kim, Y. H., Uhm, H. S., Park, G., & Choi, E. H.
850 (2014). Non-Thermal Plasma Treatment Diminishes Fungal Viability and Up-Regulates
851 Resistance Genes in a Plant Host. *Plos One*, *9*(6).
852 https://doi.org/10.1371/journal.pone.0099300
853 Peralta-Ruiz, Y., Grande Tovar, C., Sinning-Mangonez, A., Bermont, D., Pérez Cordero, A.,
854 Paparella, A., & Chaves-López, C. (2020). Colletotrichum gloesporioides inhibition using
855 chitosan-Ruta graveolens L essential oil coatings: Studies in vitro and in situ on Carica papaya
856 fruit. *International Journal of Food Microbiology*, *326*(October 2019), 108649.

https://doi.org/10.1016/j.ijfoodmicro.2020.108649

Popelář ová, E., Vlková, E., Švejstil, R., & Kouřimská, L. (2021). *The Effect of Microwave Irradiation on the Representation and Growth of Moulds in Nuts and Almonds* (p. 11). https://doi.org/doi.org/ 10.3390/foods11020221

Salo, J. M., Kedves, O., Mikkola, R., Kredics, L., Andersson, M. A., Kurnitski, J., & Salonen, H. (2020). Detection of Chaetomium globosum, Ch. cochliodes and Ch. rectangulare during the diversity tracking of mycotoxin-producing chaetomium-like isolates obtained in buildings in Finland. *Toxins*, *12*(7), 1–22. https://doi.org/10.3390/toxins12070443

Sanzani, S. M., Gallone, T., Garganese, F., Caruso, A. G., Amenduni, M., & Ippolito, A. (2019). Contamination of fresh and dried tomato by Alternaria toxins in southern Italy. *Food Additives and Contaminants - Part A Chemistry, Analysis, Control, Exposure and Risk Assessment*, *36*(5), 789–799. https://doi.org/10.1080/19440049.2019.1588998

Serhat Turgut, S., Küçüköner, E., & Karacabey, E. (2018). Improvements in drying characteristics and quality parameters of tomato by carbonic maceration pretreatment. *Journal of Food Processing and Preservation*, *42*(2), 1–12. https://doi.org/10.1111/jfpp.13282

Simoncelli, E., Schulpen, J., Barletta, F., Laurita, R., Colombo, V., Nikiforov, A., & Gherardi, M. (2019). UV-VIS optical spectroscopy investigation on the kinetics of long-lived RONS produced by a surface DBD plasma source. *Plasma Sources Science and Technology*, *28*(9). https://doi.org/10.1088/1361-6595/ab3c36

Sohail, M., Ayub, M., Ahmad, I., Ali, B., & Dad, F. (2011). Physicochemical and microbiological evaluation of sun dried tomatoes in comparison with fresh tomatoes. *J. Biochem. Mol. Biol*, *44*(3), 106–109.

Suleiman, M., Nuntah, L., Muhammad, H., Mailafiya, S., Makun, H., Saidu, A., Apeh, D., & Iheanacho, H. (2017). Fungi and Aflatoxin Occurrence in Fresh and Dried Vegetables Marketed in Minna, Niger State, Nigeria. *Journal of Plant Biochemistry & Physiology*, *05*(01), 1–4. https://doi.org/10.4172/2329-9029.1000176

Wang, P., He, J., Sun, Y., Reynolds, M., Zhang, L., Han, S., Sui, H., & Lin, Y. (2017). Display of fungal hydrophobin on the Pichia pastoris cell surface and its influence on Candida antarctica lipase B. *HHS Public Access*, *100*(13), 5883–5895. https://doi.org/10.1007/s00253-016-7431-x.Display

Wang, Y., Li, B., Shang, H., Ma, R., Zhu, Y., Yang, X., Ju, S., Zhao, W., Sun, H., Zhuang, J., Jiao,

Z. (2022). Effective inhibition of fungal growth, deoxynivalenol biosynthesis and pathogenicity in cereal pathogen Fusarium spp. by cold atmospheric plasma, Chemical Engineering Journal, 437(1), 135307. https://doi.org/10.1016/j.cej.2022.135307.

Weller, R., Price, R. J., Ormerod, A. D., & Benjamin, N. (2001). Antimicrobial effect of acidified nitrite on dermatophyte fungi, Candida and bacterial skin pathogens. *Journal of Applied Microbiology*, *90*(4), 648–652. https://doi.org/10.1046/j.1365-2672.2001.01291.x

Wu, Y., Li, J., Yang, H., & Shin, H.-J. (2017). Fungal and mushroom hydrophobins: A review. *Journal of Mushroom*, *15*(1), 1–7. https://doi.org/10.14480/jm.2017.15.1.1

van Boekel, M. A. J. S. (2008). *Kinetic modeling of reactions in foods*. CRC Press/Taylor and Francis.

Zorlugenç, B., Kiroğlu Zorlugenç, F., Öztekin, S., & Evliya, I. B. (2008). The influence of gaseous ozone and ozonated water on microbial flora and degradation of aflatoxin B1 in dried figs. *Food and Chemical Toxicology*, *46*(12), 3593–3597. https://doi.org/10.1016/j.fct.2008.09.003

- *A. niger*, *A. tubingensis,* were most abundant species in dried tomatoes.
- CAP reduced the fungal contamination on the dried tomatoes by 76.5 %.
- *A. niger* and *A. flavus* spores were more resistant ones to CAP.
- *A. chevalieri* spores were inactivated after 0.1 min of CAP-NOx.
- Spore hydrophobicity was correlated with the spore resistant to CAP.

Conflict of Interest Form

Declarations of interest

The authors of the present paper "Cold Atmospheric plasma treatment trigger changes in Sundried tomatoes mycobiota by inducing changes spore surface structure and hydrophobicity of *Aspergillus* species", Junior Bernardo Molina-Hernandez, Silvia Tappi, Matteo Gherardi, Riccardo de Flaviis, Jessica Laika, Yeimmy Yolima Peralta-Ruiz, Antonello Paparella and Clemencia Chaves-López **don't have any conflict of interest**

CRediT authorship contribution statement

Junior Bernardo Molina-Hernandez: Conceptualization, Methodology, Software, Validation, Formal analysis, Investigation, Writing – original draft, **Silvia Tappi**: Methodology, Formal analysis, Writing – review & editing; **Matteo Gherardi**: Methodology, Formal analysis, Writing –review & editing**; Riccardo de Flaviis**: Methodology, Data curation, **Jessica Laika**: Investigation, Formal analysis, **Yeimmy Yolima Peralta-Ruiz:** Investigation, review & editing, **Antonello Paparella:** Supervision, Writing – review & editing**: Clemencia Chaves-López**: Conceptualization, Supervision, Writing – original draft, Project administration.

Table 1. Primers used for PCR assay

Table 2. Absorption cross-sections in cm^2 of the species of interest at each selected wavelength.

Table 3. Estimated and calculated parameters from germination kinetics. Different letters in the same column indicate significant differences ($p < 0.05$) according to LSD post-hoc test. Goodness of fit indexes were reported as mean ± standard deviation.

Table 4. Textural values in sundried tomatoes untreated and treated with CAP treatments.

Table S1. Identification of the fungi isolates form dry tomatoes, determined by amplifying Internal transcribed spacer 1 (ITS1) and ITS2 regions and the 5.8S ribosomal DNA (rDNA) region, β-tubulin and Calmodulin gene and nucleotide sequences.

Figure 1. Values of NO_2 after different treatment times. The values are the mean of three repetitions. In each panel, data are mean ± SD, and statistical significance is specified with letters (*$p \leq 0.05$ as determined by paired Student t-test).

Figure 2. Frequency of the filamentous fungi isolated on the surface of sundried tomatoes belonging to different batches. Created with Datawrapper.

Figure 3. Kinetics of germination reduction in five different fungal spores, as a function of time of treatment, fitted by the Weibull reparametrized model. Dots indicate real data as means of three replications. The regression parameters were listed in Table 3.

Figure 4. Microscopic visualization of *A. chevalieri* PSJ144, *A. tubingensis* PSJ100, *A. alternata* PSJ77, A. flavus PSJ30 and *A. niger* PSJ38 spores before and after treatment with CAP-NOx. Scale bars, 10 μm.

Figure 5. Confocal laser scanning microscopy analysis of cell viability in *A. chevalieri* PSJ144, *A. tubingensis* PSJ100*, A. alternata* PSJ77*, A. flavus* PSJ30, and *A. niger* PSJ 38 after treatment with CAP-NOx. Cells were stained with green fluorescence CFDA (carboxyfluorescein diacetate) and red propidium iodide (PI) dyes. Bars indicate the percentage of cell live (green) and death (red) spore. Image zoom of spores indicate a total loss of viability after treatment with CAP-NOx. Scale bar 10 um.

Figure 6. Analysis of the surface hydrophobicity of the *A. niger* PSJ38 (a); *A. flavus* PSJ30 (b); *A. chevalieri* PSJ144(c); *A. tubingensis* PSJ100(d), and *A. alternata* PSJ77(e) after treatment with CAP-NOx. Data were obtained from three independent experiments. Different letters represent significant differences among the sample ($p < 0.05$; Tukey HSD post-hoc test).

Figure S1. Individually plots of germination kinetics in five different fungal spores for three replicates fitted by the Weibull reparametrized model. Dots indicate real data. X axis and Y axis indicate time of treatment and percentage of germination respectively.

Figure

Click here to access/download;Figure;Figure 1.pdf

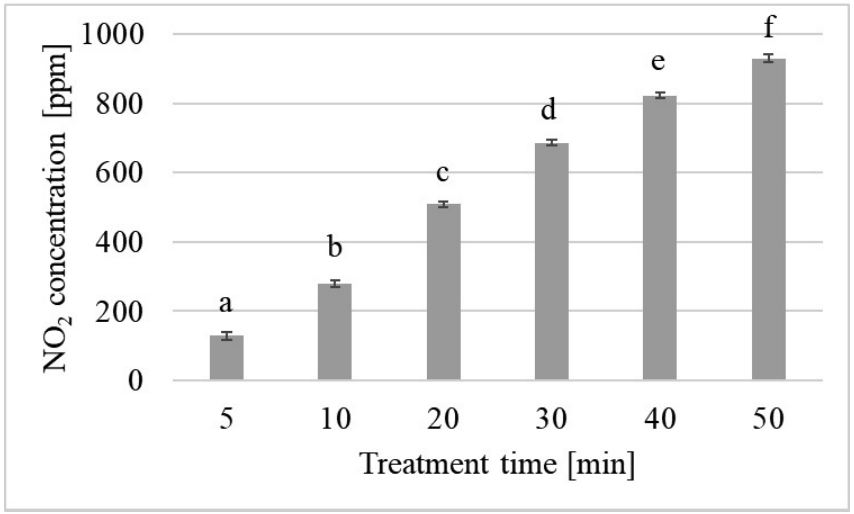

Figure

Click here to access/download;Figure;Figure 2.pdf

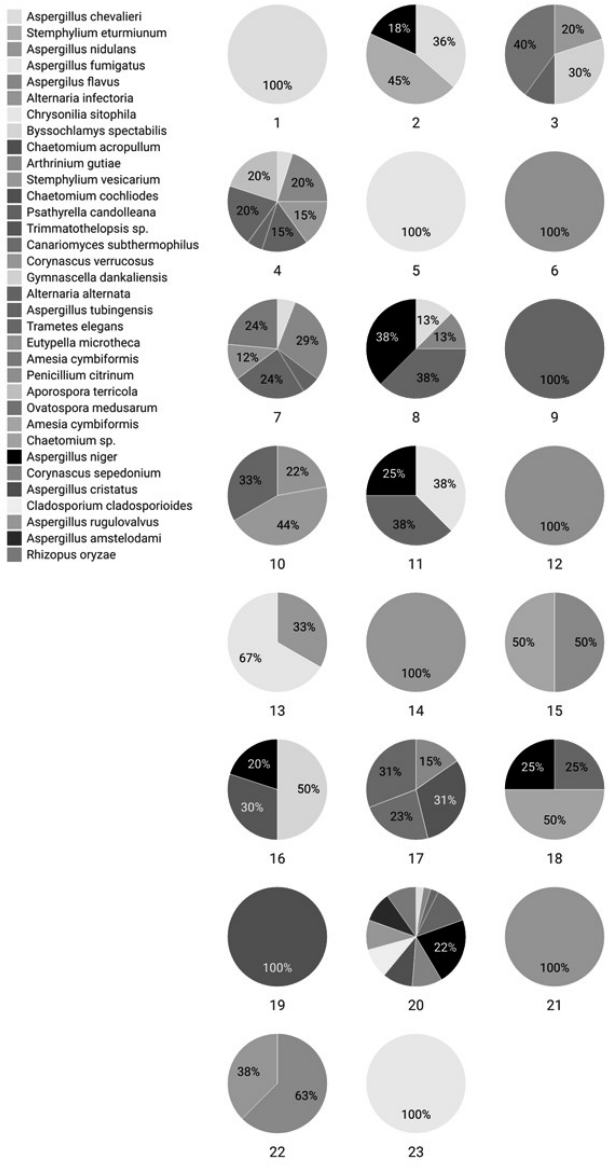

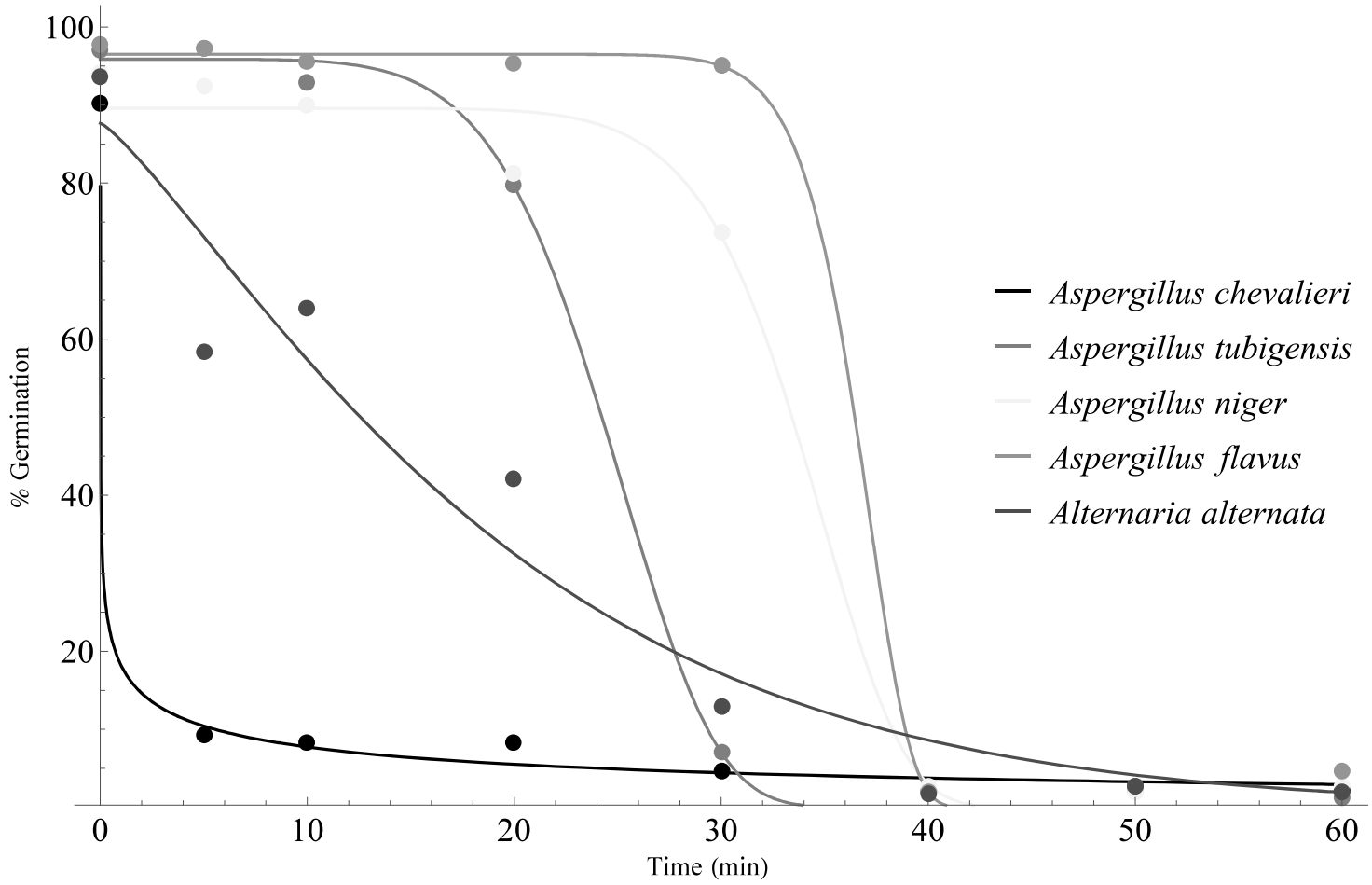

Figure

Click here to access/download;Figure;Figure 4.pdf

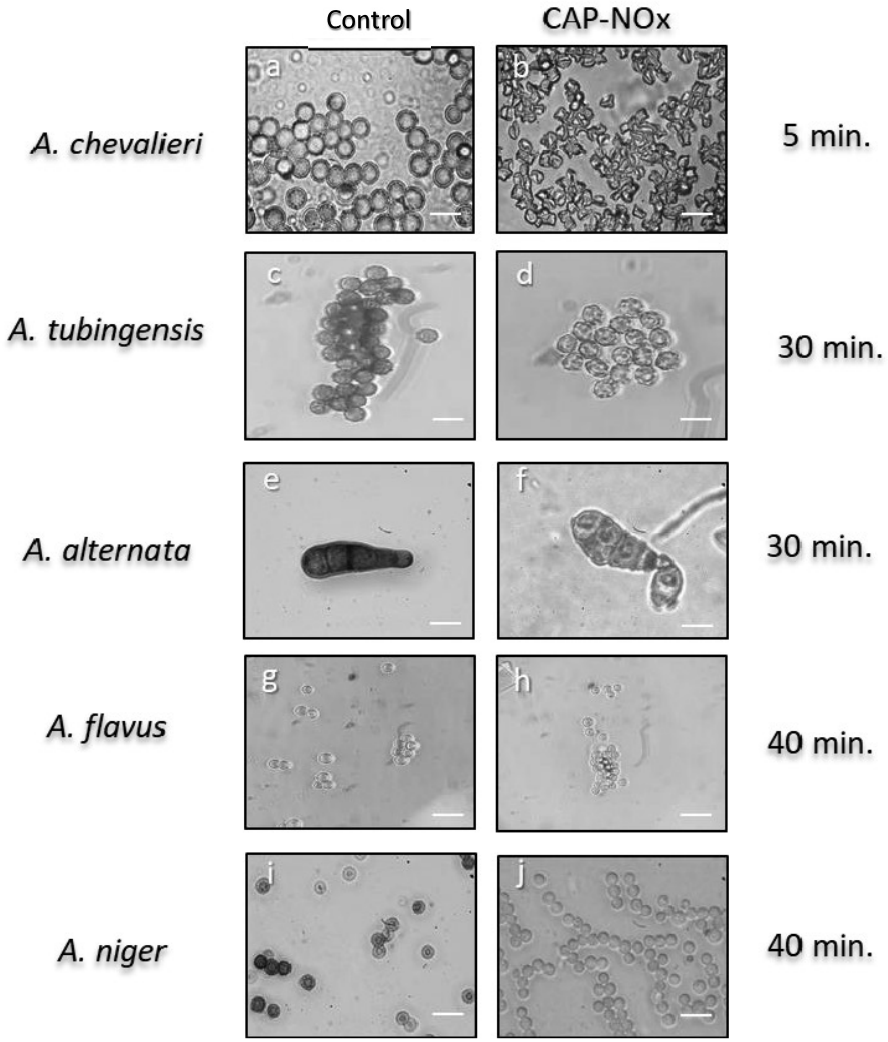

Figure

Click here to access/download;Figure;Figure 5.pdf

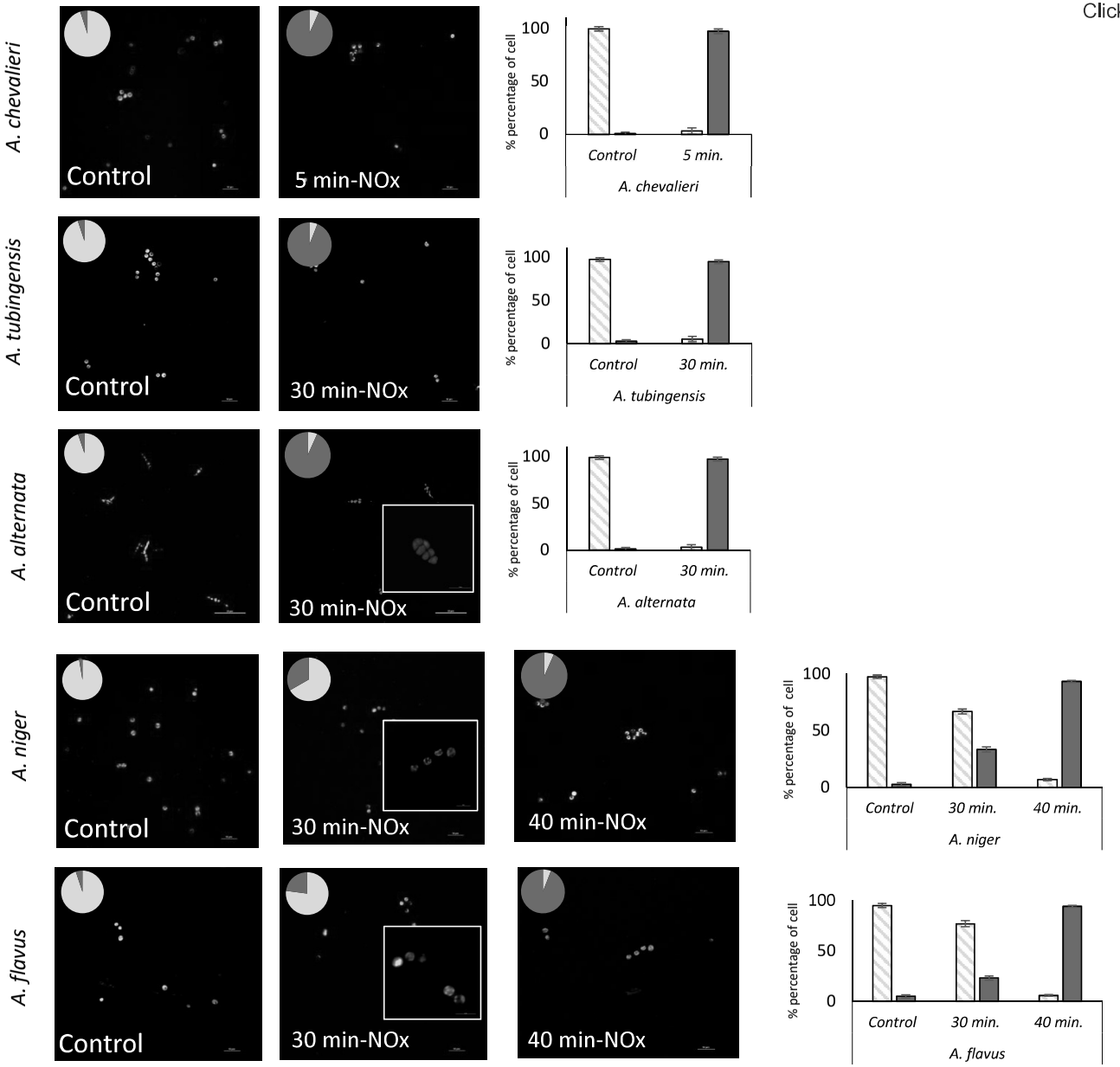

Figure

Click here to access/download;Figure;Figure 6.pdf

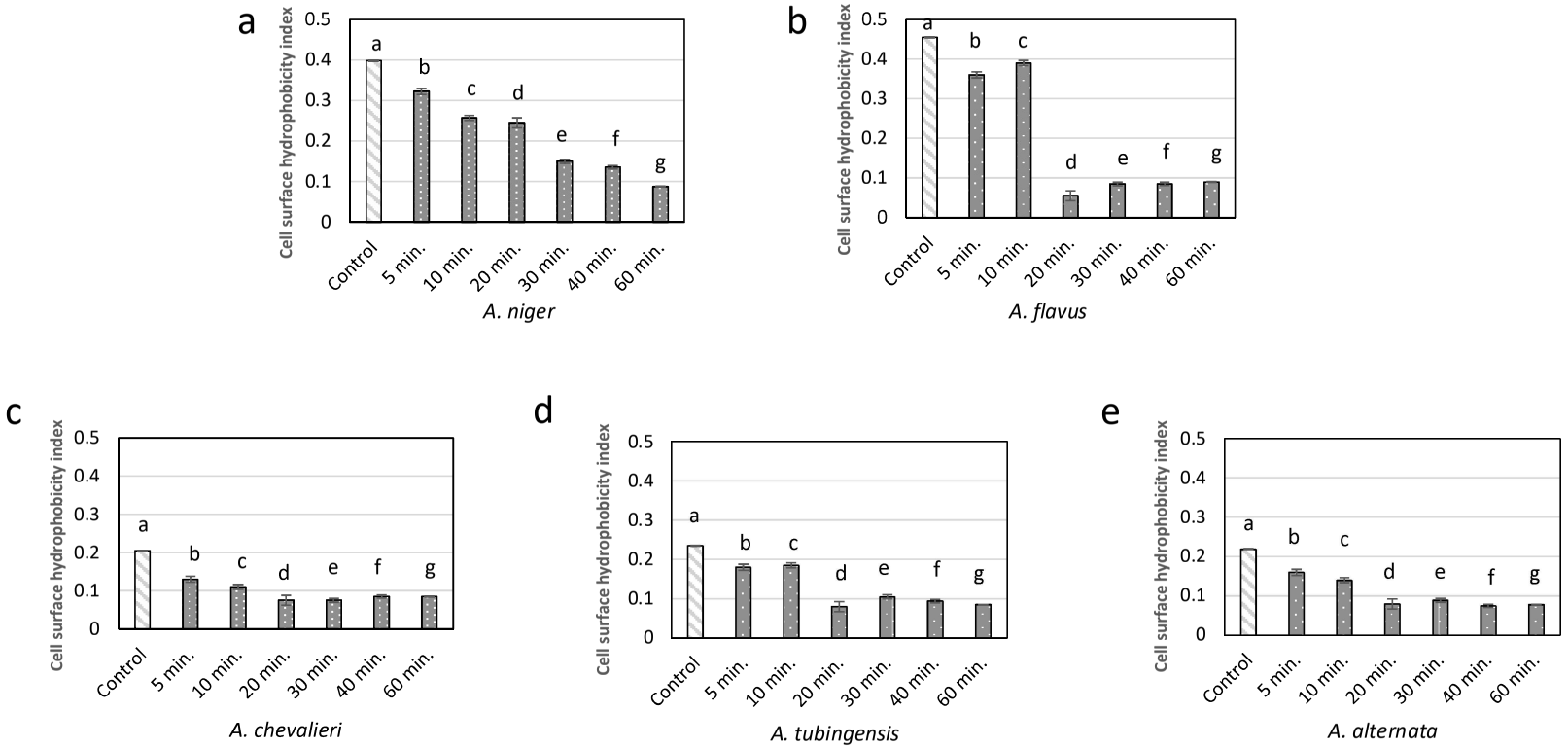

Table 1. Primers used for PCR assay.

Gene name	Gene	Length bp	Primer	Sequences (5′→ 3′)	Reference
Internal transcribed spacer 1 (ITS1) and ITS2 regions and the 5.8S ribosomal DNA (rDNA) region	**ITS (1-4)**	420-825	ITS1 (F)	**5′TCCGTAGGTGAACCTGCGG3′**	(Glass & Donaldson, 1995)
			ITS4 (R)	**5′TCCTCCGCTTATTGATATGC3′**	
	ITS (1-2)	565-613	ITS1 (F)	**5′ GGAAGTAAAGTCGTAACAAGG 3′**	
			ITS2 (R)	**5′ TTGGTCCGTGTTTCAAGACG 3′**	
β-tubulin	**ben A**	1125	β-tub 2a (F)	**5′GGTAACCAAATCGGTGCTTTC 3′**	(Makhlouf et al., 2019)
			β-tub 2b (R)	**5′ACCCTCAGTGTAGTGACCCTTGGC 3′**	
Calmodulin	**cmdA**	543	Cmd5 (F)	**5′-CCGAGTACAAGGAGGCCTTC-3′**	
			Cmd6 (R)	**5′-CCGATAGAGGTCATAACGTGG-3′**	

Abbreviation: F: Forward, R: Reverse

Table 2. Absorption cross-sections in cm^2 of the species of interest at each selected wavelength.

Selected wavelength	**O_3 cross-section**	**NO_2 cross-section**
253±1.2 nm	(1.12±0.02)E-17	(1.1±0.3)E-20
400±1.2 nm	(1.12±0.08)E-23	(6.4±0.2)E-19

Table 3. Estimated and calculated parameters from germination kinetics. Different letters in the same column indicate significant differences ($p < 0.05$) according to LSD post-hoc test. Goodness of fit indexes was reported as mean ± standard deviation.

	Estimated parameters[1]			Calculated parameter[2]		Goodness of fit		
	N_0 (%)	μ_β (%/min)	β (min)	μ_{max} (%/min)	λ (min)	R^2	CV(RMSD)	AIC
Aspergillus flavus	96.5^{a}	17.8^{ab}	37.2^{a}	17.9^{a}	33.8^{a}	0.999 ± 0.000	3.38 ± 0.15	43.09 ± 0.82
Aspergillus niger	89.6^{b}	9.2^{ab}	35.3^{b}	9.2^{b}	29.2^{b}	0.997 ± 0.000	6.55 ± 0.33	51.91 ± 0.54
Aspergillus tubigensis	95.9^{a}	8.9^{ab}	25.9^{c}	9.0^{b}	19.1^{c}	0.999 ± 0.000	3.74 ± 0.40	40.59 ± 1.75
Alternaria alternata	87.5^{b}	2.0^{b}	20.2^{d}	3.3^{c}	0.7^{d}	0.975 ± 0.003	21.91 ± 1.25	63.88 ± 0.39
Aspergillus chevalieri	90.3^{b}	152.1^{a}	0.1^{e}	$\rightarrow\infty$[3]	0[3]	0.998 ± 0.000	8.65 ± 1.01	36.59 ± 1.84

[1] Computed by fitting Eq. 1.

[2] Computed by using Eq. 2 and 3.

[3] Values theoretically assigned, since it is impossible to calculate these parameters when no inflection point is present.

Table 4. Textural values in sundried tomatoes untreated and treated with CAP treatments.

Property	Control	5 min.	10 min.	20 min.	30 min.
Firmness	483.3±133.1[a]	426.0±104.9[a]	606.6±124.8[b]	252.5±139.8[c]	426.0±104.9[c]
Skin Strenght	1325.8±460.7[a]	1307.3±202.3[a]	1319.0±353.5[a]	823.4±521.5[b]	1697.5±161.4[c]
Elasticity	5.7±2.7[a]	6.5±1.0[a]	6.5±1.6[a]	6.1±2[a]	7.6±1.8[b]

[a,b,c] Means in the same row with different superscripts are significantly different (P 0.05).

Table S1. Identification of the fungi isolates form dry tomatoes, determined by amplifying Internal transcribed spacer 1 (ITS1) and ITS2 regions and the 5.8S ribosomal DNA (rDNA) region, β-tubulin and Calmodulin gene and nucleotide sequences.

Sample	Closed relative	Primer	Identity %	Accession number
PSJ 77	*Alternaria alternata*	*ITS1-ITS4*	*100*	*KF881759.1*
PSJ 65		*ITS1-ITS4*	*100*	*KF881759.1*
PSJ 79		*ITS1-ITS4*	*100*	*KF881759.1*
PSJ 70	*Alternaria infectoria*	*ITS1-ITS4*	*100*	*MK226292.1*
PSJ 70-1		*ITS1-ITS4*	*100*	*MK226292.1*
PSJ 74	*Amesia cymbiformis*	*ITS1-ITS4*	*100*	*MH861721.1*
PSJ 72	*Aporospora terricola*	*ITS1-ITS4*	*99*	*AF049088.1*
VJT-20	*Aspergillus amstelodami*	*βt2a-βt2b*	*99,7*	FR775356.2
PSJ-76-1	*Aspergillus chevalieri*	*ITS1-ITS4*	*100*	*MT316337.1*
PSJ 79		*ITS1-ITS4*	*100*	*MT316337.1*
PSJ 132-1		*ITS1-ITS4*	*100*	*MN174037.1*
PSJ 150		*ITS1-ITS4*	*100*	*MN174037.1*
PSJ 131		*ITS1-ITS4*	*100*	*MN174037.1*
PSJ 144		*ITS1-ITS4*	*99*	*MT316339.1*
VJT-2	*Aspergillus cristatus*	*ITS1-ITS4*	*99,32*	KY828916.2
PSJ 30	*Aspergillus flavus*	*ITS1-ITS2*	*99*	*JX501356.1*
PSJ 14		*ITS1-ITS4*	*99*	*MT645322.1*
PSJ 106		*ITS1-ITS4*	*100*	*MT558941.1*
PS154		*ITS1-ITS4*	*100*	*MT292809.1*
PSJ 40-1	*Aspergillus fumigatus*	*ITS1-ITS4*	*99*	*MF379664.1*
PSJ 9		*ITS1-ITS4*	*100*	*MK841416.1*
PSJ 10		*ITS1-ITS4*	*99*	*MT487775.1*
PSJ 50		*ITS1-ITS4*	*100*	*OK067466.1*
PSJ 48	*Aspergillus nidulans*	*ITS1-ITS4*	*100*	*MK397763.1*
PSJ 105		*ITS1-ITS4*	*99*	*MT316339.1*
VJT 7	*Aspergillus niger*	*CMD5-CMD6*	*99,6*	HQ632731.1
VJT 14		*βt2a-βt2b*	*99,7*	MN907662.1
VJT 12		*ITS1-ITS4*	*99,1*	MN493772.1
VJT 28		*ITS1-ITS4*	*99,1*	LC577101.1
VJT 15		*βt2a-βt2b*	*99,7*	JX545078.1
VJT 18		*ITS1-ITS4*	*99,1*	MTI23512.1
VJT 1		*βt2a-βt2b*	*99,12*	MT597823.1
VJT 6		*βt2a-βt2b*	*98,8*	KY990205.1
VJT 17		*βt2a-βt2b*	*99,7*	KU865178.1
VJT 26		*ITS1-ITS4*	*98*	*MK138359.1*
PSJ 38		*βt2a-βt2b*	*99.1*	*KJ36066.1*
		CMD5-CMD6	*99.1*	*MH447369.1*
VJT-5	*Aspergillus rugulovalvus*	*βt2a-βt2b*	*100*	AB248319.1
PSJ 100	*Aspergillus tubingensis*	*CMD5-CMD6*	*100*	*MK166185.1*
PSJ 109		*CMD5-CMD6*	*100*	*KY612372.1*
VJT 10		*CMD5-CMD6*	*98,9*	KY612372.1
VJT 30		*CMD5-CMD6*	*98,9*	KX231824.1
VJT 8		*ITS1-ITS2*	*100*	*KY612372.1*
VJT 16		*ITS1-ITS4*	*100*	MK166185.1
PSJ 16		*βt2a-βt2b*	*98,9*	MK166185.1
PSJ 12	*Arthrinium gutiae*	*ITS1-ITS4*	*100*	*MN634560.1*
PSJ 143		*ITS1-ITS4*	*100*	*MN634560.2*
PSJ 13	*Byssochlamys spectabilis*	*ITS1-ITS4*	*99*	*MW335157.1*
PSJ 140	*Canariomyces subthermophilus*	*ITS1-ITS4*	*98*	*MK926804.1*
PSJ 135	*Chaetomium cochliodes*	*ITS1-ITS4*	*100*	MH590621.1
PSJ 40	*Chaetomium acropullum*	*ITS1-ITS4*	*99*	*MH550490.1*
PSJ 40-2		*ITS1-ITS4*	*99*	*KU571511.1*
PSJ 83		*ITS1-ITS4*	*99*	*KU571511.1*
PSJ 119	*Corynascus verrucosus*	*ITS1-ITS4*	*100*	*KY065360.1*
PSJ 15	*Chrysonilia sitophila*	*ITS1-ITS4*	*98*	*GU192459.1*
PSJ 15-1		*ITS1-ITS4*	*99.9*	*GU192459.1*
VJT-4	*Corynascus sepedonium*	*ITS1-ITS4*	*99,43*	MK919294.1
VJT-3	*Cladosporium cladosporioides*	*ITS1-ITS4*	*99,3*	KY039309.1

PSJ 55	*Eutypella microtheca*	*ITS1-ITS4*	*99*	*MF359643.1*
PSJ 96		*ITS1-ITS4*	*100*	*MH864886.1*
PSJ 98		*ITS1-ITS4*	*99*	*MH864886.1*
PSJ 151	*Gymnascella dankaliensis*	*ITS1-ITS4*	*100*	*AY304514.1*
PSJ 86	*Penicillium citrinum*	*ITS1-ITS4*	*99*	*MN418435.1*
PSJ 70		*ITS1-ITS4*	*99*	*MG575517.1*
PSJ 73		*ITS1-ITS4*	*100*	*LC514694.1*
PSJ 76	*Ovatospora medusarum*	*ITS1-ITS4*	*100*	*MH860651.1*
PSJ 110	*Psathyrella candolleana*	*ITS1-ITS4*	*99*	*MT424873.1*
VJT-22	*Rhizopus oryzae*	*ITS1-ITS4*	*99,7*	LC514326.1
VJT-25		*ITS1-ITS4*	*99,7*	MT603963.1
VJT 11		*ITS1-ITS4*	*99,6*	LC514321.1
PSJ 87-1	*Stemphylium eturmiunum*	*ITS1-ITS4*	*100*	*MW883450.1*
PSJ 3	*Stemphylium vesicarium*	*ITS1-ITS4*	*100*	*MG065802.1*
PSJ 51		*ITS1-ITS4*	*100*	*MG065802.1*
PSJ 102		*ITS1-ITS4*	*100*	*MW245000.1*
PSJ 81		*ITS1-ITS4*	*100*	*MN328401.1*
PSJ 58	*Trametes elegans*	*ITS1-ITS4*	*100*	*MT597442.1*
PSJ 137	*Trimmatothelopsis sp.*	*ITS1-ITS4*	*95*	*MK948457.1*